CHAPTER IV

RESULTS AND DISCUSSION

This chapter focuses on the development of microsystems with electrochemical detectors that are suitable for the detection of environmentally important toxic metal ions. The optimized conditions are established for separating cationic species. The separation of lead(II), cadmium(II) and copper(II) ions in aqueous solution is optimized using a coion to modify the electrophoretic mobilities of the ions. Some significant examples are discussed in the following sections, combining the versatility of microchips with the simplicity of electrochemical detectors to automate, miniaturize, and simplify both analytical tools and processes to solve analytical problems in an efficient and convenient fashion.

Since the detection response results from the degree of coupling of the CE voltage to the oxidation potential of the sample plug and the running buffer passing through the working electrode. The difference of conductivity between the sample plug and the running buffer is an essential factor influencing the detection signal. It is well known that carrier electrolytes with low-mobility coion are preferred for analysis of small ions. 2-(N-Morpholino)ethanesulfonic acid (MES) + histidine is a typical carrier electrolyte with a low-mobility coion used for the separation of small ions. In the following sections, the influence of some experimental parameters such as: the buffer pH, concentration, separation voltage, and the detection potential were studied in detail in order to examine their effects on the separation efficiency and detection sensitivity.

4.1 Batch analysis : cyclic voltammetry

Cyclic voltammetry was initially used as a means of examining the electrochemical signal of a screen-printed carbon electrode for the analysis of three metal ions (Pb^{2+}, Cd^{2+} and Cu^{2+}), as well as dopamine and catecholamine. The results obtained from the batch analysis system will be presented.

4.1.1 Background current

The cyclic voltammetric (I-E) responses for a solution containing 25 mM MES and L-histidine at pH 7.0 (running buffer solution) is shown in Figure 4.1. The results obtained offer the corresponding background voltammogram for the screen-printed carbon working electrode as observed with a scanning range of ca. +1.0 to -1.0 V versus a Ag/AgCl reference electrode with a scan rate of 50 mV/s.
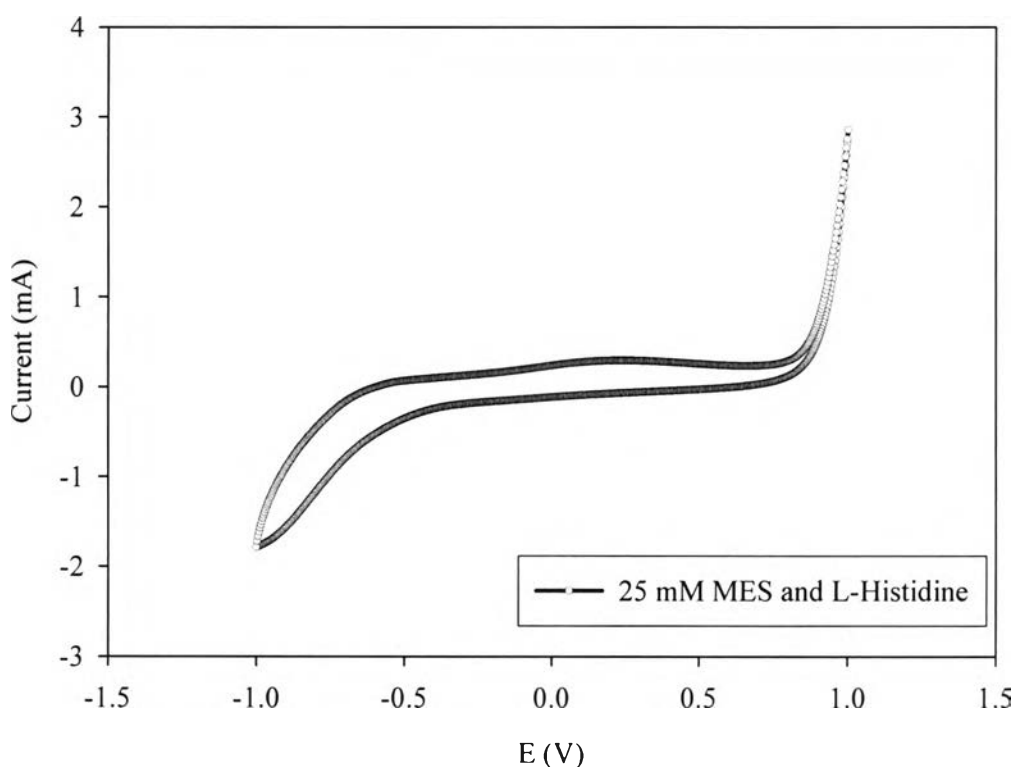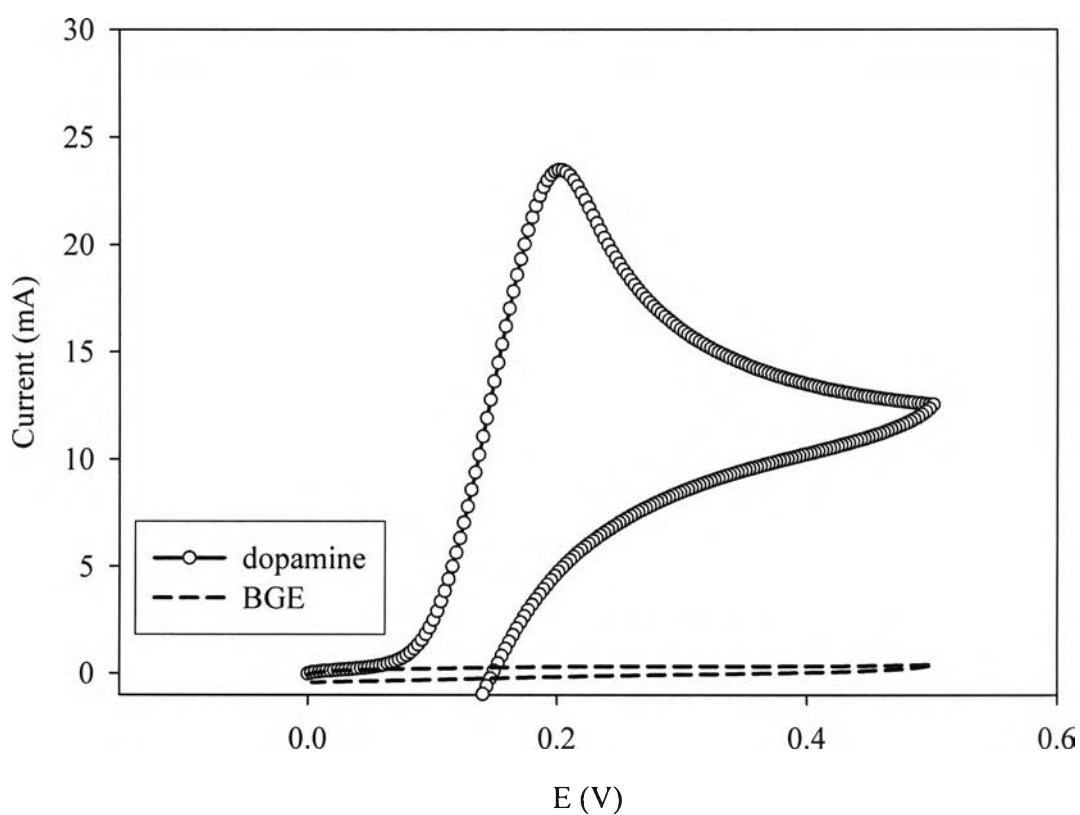

Figure 4.1 Cyclic voltammogram of 25 mM MES and L-histidine (pH 7.0) buffer at screen-printed carbon electrode. The scan rate was 50 mV/s.

4.1.2 The electrochemical characteristics of dopamine and catechol.

The cyclic voltammetry of dopamine and catechol were studied to find the oxidation peaks that was obtained at the optimal potential. This potential was used as the detection potential for microchip CE systems. The dopamine and catechol were the standard analyte for test the microchip CE systems performance.

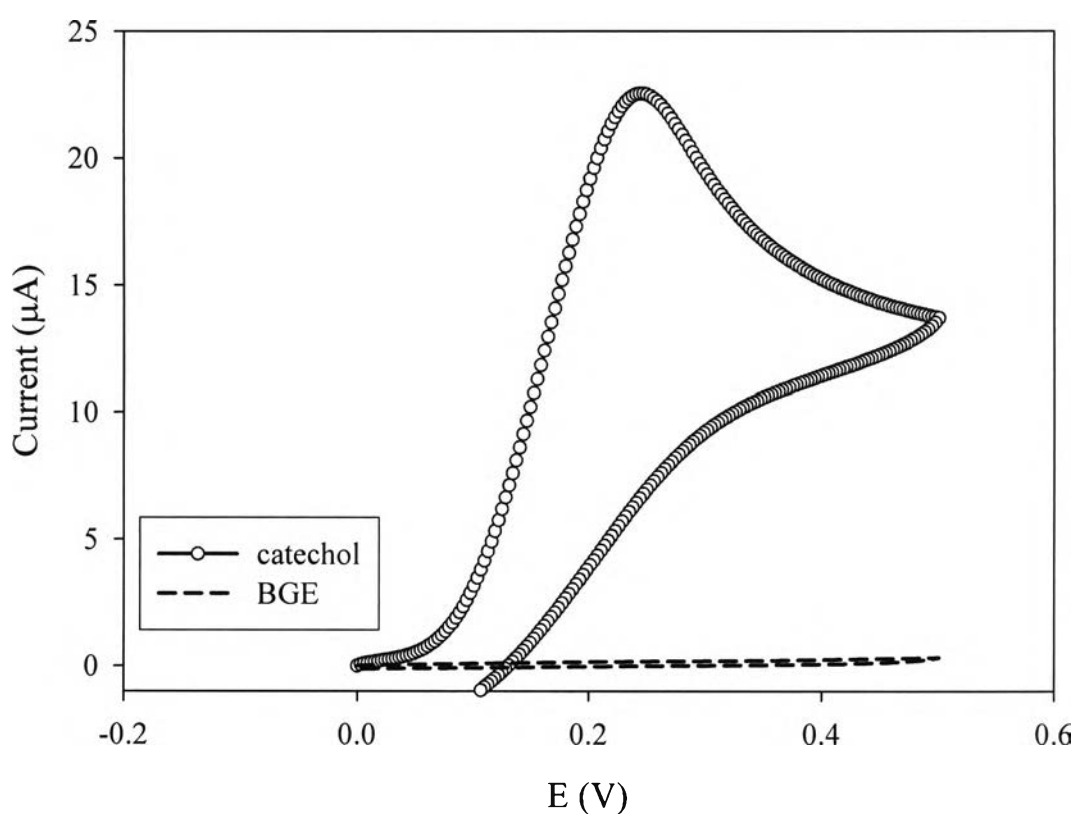### 4.1.2.1 The electrochemical signal of dopamine

The cyclic voltammograms of a solution containing 1 mM dopamine in MES and L-histidine buffer solution together with the corresponding background voltammogram at the screen-printed carbon electrode is shown in Figure 4.2. In the presence of dopamine, a response was obtained at the anodic signal that was observed on the positive scan in the region of ca. 0 to + 0.5 V versus Ag/AgCl with scan rate 50 mV/s. The voltammetric oxidation peak of dopamine was obtained at a potential of 0.2 V.

Figure 4.2 Cyclic voltammogram of 1 mM dopamine in 25 mM MES and L-histidine (pH 7.0) buffer at screen-printed carbon electrode. The scan rate was 50 mV/s.

4.1.2.2 The electrochemical signal of catechol

The studies of electrochemical response of catechol in MES and L-histidine buffer solution at screen-printed carbon electrode was investigated. The anodic signals over the potential range from 0.0 to +0.5 V with a scan rate 50 mV/s is shown in Figure 4.3. A well defined oxidation peak (with an Ep = 0.25 V versus Ag/AgCl) of catechol was observed.
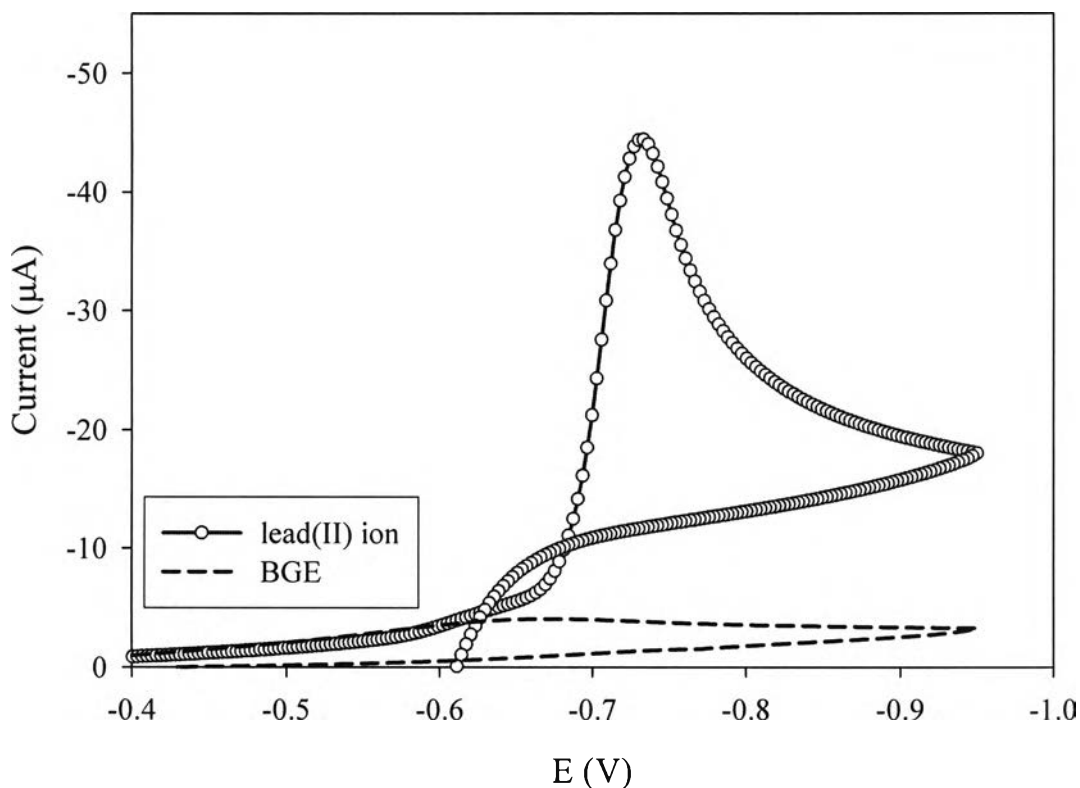

Figure 4.3 Cyclic voltammogram of 1 mM catechol in 25 mM MES and L-histidine (pH 7.0) buffer at screen-printed carbon electrode. The scan rate was 50 mV/s.

4.1.3   The electrochemical characteristics of metal ions.

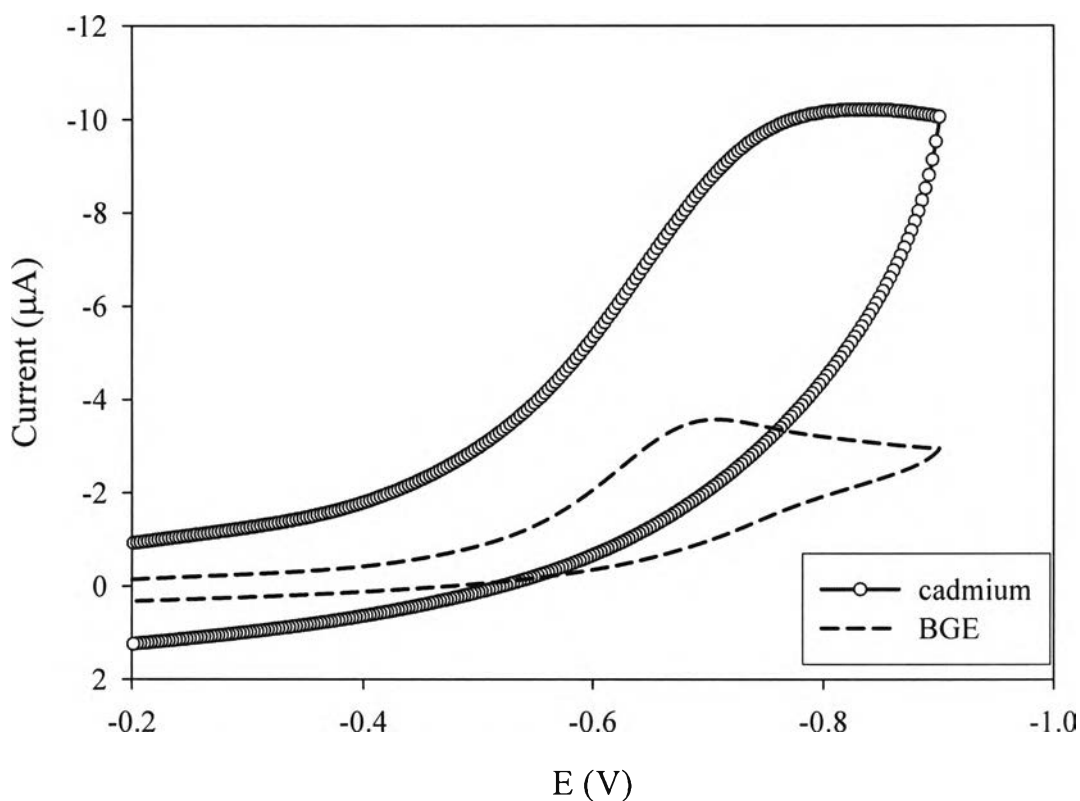#### 4.1.3.1 The electrochemical signal of lead

The study of electrochemical reduction of lead (II) ions using a screen-printed carbon electrode was performed using the MES buffer solution (pH 7.0). Figure 4.4 displays typical cyclic voltammograms of 1 mM lead in a buffer solution. The corresponding background voltammograms are also shown. An approximate, but well defined reduction (with an E_p = -0.73 V versus Ag/AgCl) was observed for lead (II) ion starting at around -0.7 volt within the investigated potential range (-0.2 to -0.95 V).

Figure 4.4 Cyclic voltammogram of 1 mM lead(II) ion in 25 mM MES and L-histidine (pH 7.0) buffer at screen-printed carbon electrode. The scan rate was 50 mV/s.

### 4.1.3.2 The electrochemical signal of cadmium

The study of electrochemical reduction of cadmium (II) ions using a screen-printed carbon electrode was performed using the MES buffer solution (pH 7.0) within the potential range from -0.2 to -0.9 V. The cyclic voltammograms of cadmium in buffer solution is shown in Figure 4.5. The corresponding background voltammograms are also shown. A well defined reduction was observed at -0.84 V versus Ag/AgCl for cadmium (II) ion.

Figure 4.5 Cyclic voltammogram of 1 mM cadmium(II) ion in 25 mM MES and L-histidine (pH 7.0) buffer at the screen-printed carbon electrode. The scan rate was 50 mV/s.

4.1.3.3 The electrochemical signal of copper

The cyclic voltammograms of copper ions in the MES buffer solution (pH 7.0) using a screen-printed carbon electrode is shown in Figure 4.6. The electrochemical reduction of copper (II) ions was obtained within a potential range from 0 to −0.95 V. The corresponding background voltammogram is also shown. A well defined reduction potential of copper (II) ions is observed at -0.62 V versus Ag/AgCl.
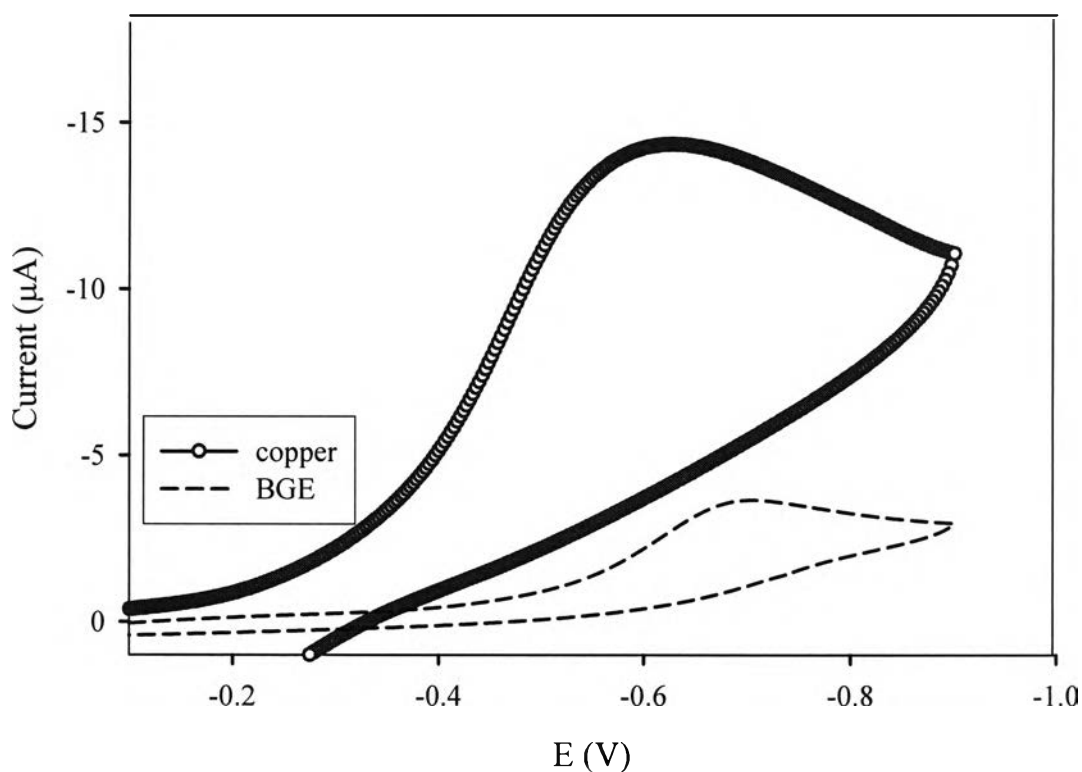
Figure 4.6 Cyclic voltammogram of 1 mM copper(II) ion in 25 mM MES and L-histidine (pH 7.0) buffer at screen-printed carbon electrode. The scan rate was 50 mV/s.

Table 4.1 Detection potential for analysis in 25 mM MES and L-histidine buffer solution with screen-printed carbon electrode.

Analyte	Potential (V)
Dopamine	+0.20
Catechol	+0.25
Lead (II)	-0.73
Cadmium (II)	-0.84
Copper (II)	-0.62

Table 4.1 was shown the detection potential for microchip CE with amperometric detection of the analytes, dopamine, catechol, lead, cadmium, and copper, in MES and L-histidine buffer solution.

4.1.4 Effect of scan rate on analytes voltammetric response

In order to verify that these oxidative reactions were diffusion controlled, a study into the effects of scan rate on the electrochemical signal was undertaken. The equation used for describing the relationship between the current signal and scan rate for a totally irreversible reaction is shown below.

$$i_p (diffusion) = (2.99 \times 10^5) n (\alpha n_a)^{1/2} A C_0 * D_0^{1/2} v^{1/2}$$

The effect of the scan rate on the electrochemical behavior of metal ions, dopamine, and catechol were investigated by varying the scan rate. The relationship between the current responses and the square root of the scan rate were observed. These results show the current response is directly proportional to the square root of the scan rate. It can be concluded that the diffusion process controls the transportation of these analytes.

### 4.1.4.1 Effect of scan rate on dopamine voltammetric response

The corresponding voltammetric responses of dopamine was investigated by varying the scan rate. The results are shown in Figure 4.7, displaying the cyclic voltammograms recorded during variation of the scan rate for the screen-printed carbon electrode. It can be seen that the peak current was linearly proportional to the square root of the scan rate within the range of 10 to 300 mV/s. The linear regression analysis yields $R^2 > 0.9990$. From the voltammogram, it was found that the peak potential shifted positively with increasing sweep rate, as expected for an irreversible process, and the linearity suggests that the reaction involves a diffusing species.
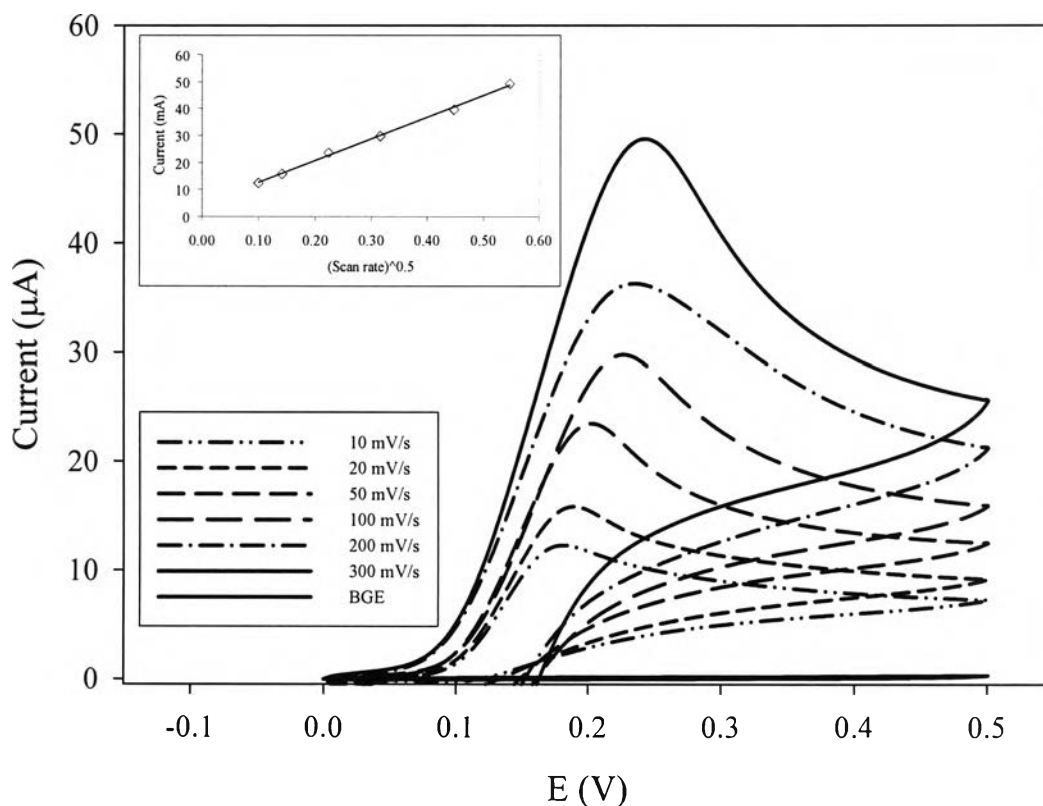
Figure 4.7 Cyclic voltammogram of 1 mM dopamine in 25 mM MES and L-histidine (pH 7.0) buffer at the screen-printed carbon electrode. The scan rate was from 10-300 mV/s. The relationship of the current signal to the square root of the scan rate is shown in the Figure inset.

### 4.1.4.2 Effect of scan rate on catechol voltammetric response

The corresponding voltammetric response of catechol was investigated by variation of the scan rate. Figure 4.7 displays the cyclic voltammograms recorded during variation of the scan rate for the screen-printed carbon electrode. From the voltammogram, it was found that the peak potential shifted positively with increasing sweep rate. It can be seen that the peak current is linearly proportional to the square root of the scan rate within the range of 10 to 300 mV/s. The results are as expected for an irreversible process. The linear regression analysis yields an $R^2 > 0.9990$. This linearity suggests that the reaction is controlled by diffusion process of catechol.
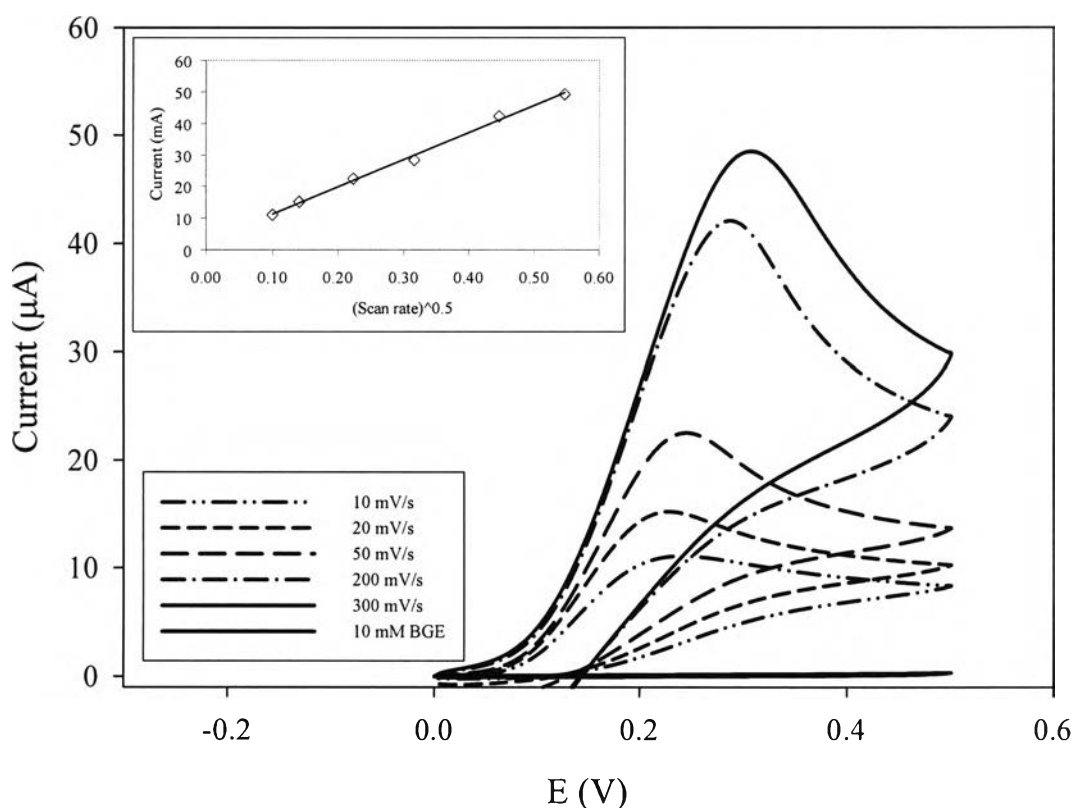
Figure 4.8 Cyclic voltammogram of 1 mM catechol in 25 mM MES and L-histidine (pH 7.0) buffer at screen-printed carbon electrode. The scan rate was between 10-300 mV/s. The relationship of current signal and square root of scan rate was also shown in this Figure (inset).

### 4.1.4.3 Effect of scan rate on lead(II) voltammetric response

The effect of the scan rate on the electrochemical behavior of lead(II) was obtained. The cyclic voltammograms recorded during variation of the scan rate, within the range 10 to 300 mV/s for the screen-printed carbon electrode are shown in Figure 4.9. The corresponding voltammetric responses displayed the oxidation of analytes underwent is an irreversible reaction. The relationship between the current response and the square root of the scan rate for lead ion is shown in the inset. From these results, the current response of the lead ion was directly proportional to the square root of the scan rate. It can be concluded that the diffusion process controls the transportation of this analyte.
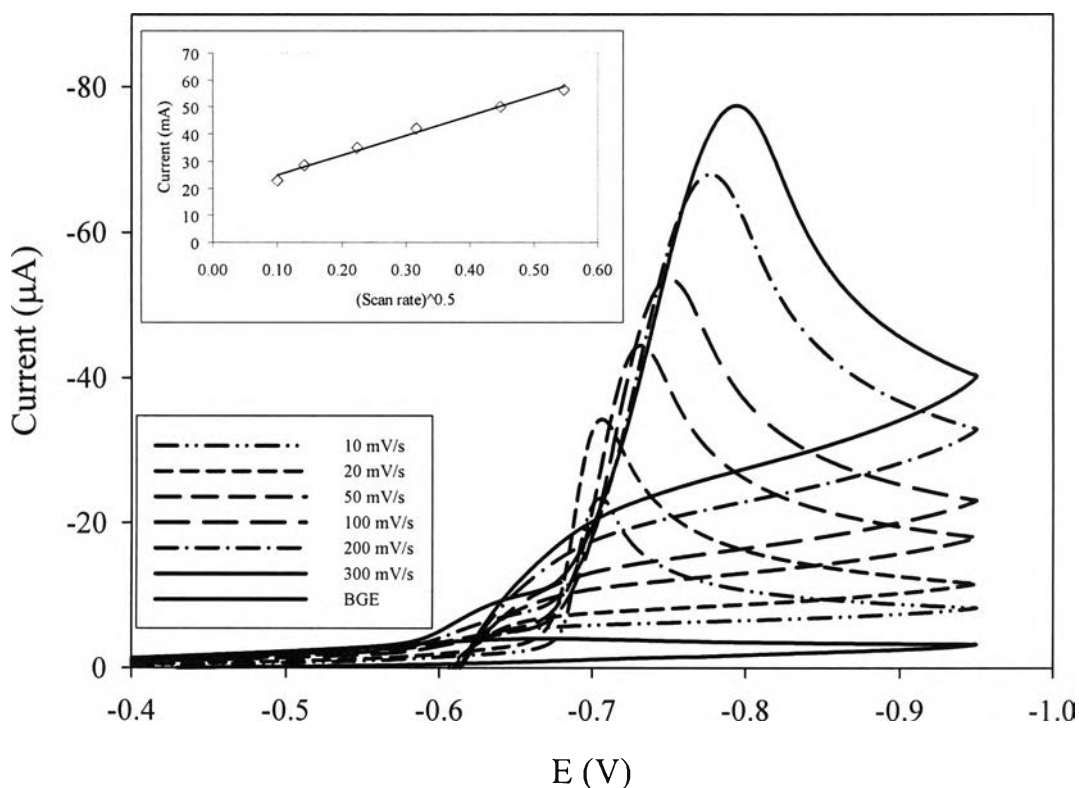
Figure 4.9 Cyclic voltammogram of 1 mM lead in 25 mM MES and L-histidine (pH 7.0) buffer at screen-printed carbon electrode. The scan rate was 10-300 mV/s. The relationship of current signal and square root of scan rate is also shown in this Figure(inset).

#### 4.1.4.4 Effect of scan rate on cadmium(II) voltammetric response

The electrochemical behavior of cadmium(II) in MES and L-histidine using the screen-printed carbon electrode during variation of the scan rate was obtained. Figure 4.10 shows the cyclic voltammograms recorded within the scan rate range of 10 to 300 mV/s. It can be seen that peak current is linearly proportional to the square root of the scan rate. The linear regression analysis yields an $R^2 > 0.9990$. From the voltammogram, it was found that the peak potential shifted positively with increasing sweep rate, as expected for an irreversible process, and the linearity suggests that the reaction involves the diffusion controlled transportation of cadmium.
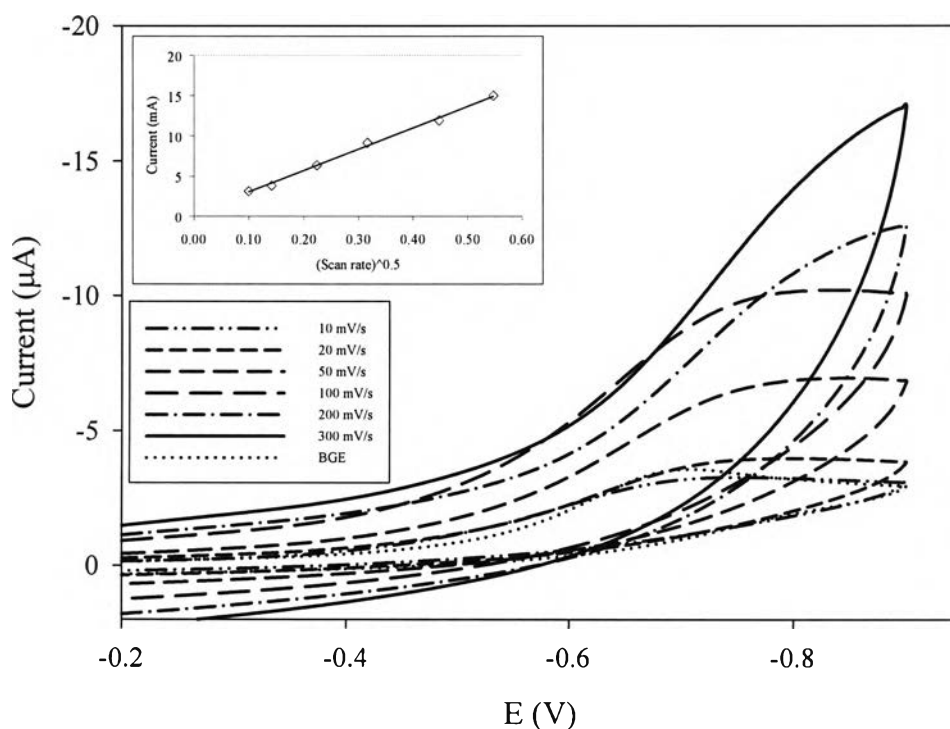
Figure 4.10 Cyclic voltammogram of 1 mM cadmium in 25 mM MES and L-histidine (pH 7.0) buffer at screen-printed carbon electrode. The scan rate was 10-300 mV/s. The relationship of current signal and square root of scan rate is also shown in this Figure (inset).

4.1.4.5 Effect of scan rate on copper(II) voltammetric response

The corresponding voltammetric response varied with scan rate with the current plateau increasing linearly with the square root of the scan rate. Such dependence indicates that the reduction of copper(II) is indeed diffusion controlled. Figure 4.11 shows the cyclic voltammograms of this metal in MES and L-histidine when using the screen-printed carbon electrode, as recorded with scan rates between 10 and 300 mV/s. It can be seen that peak current is linearly proportional to the square root of the scan rate. The linear regression analysis yields $R^2 > 0.9990$. From the voltammogram, it was found that the peak potential shifted positively with increasing sweep rate, as expected for an irreversible process, and the linearity suggests that the reaction involves diffusion controlled transportation.
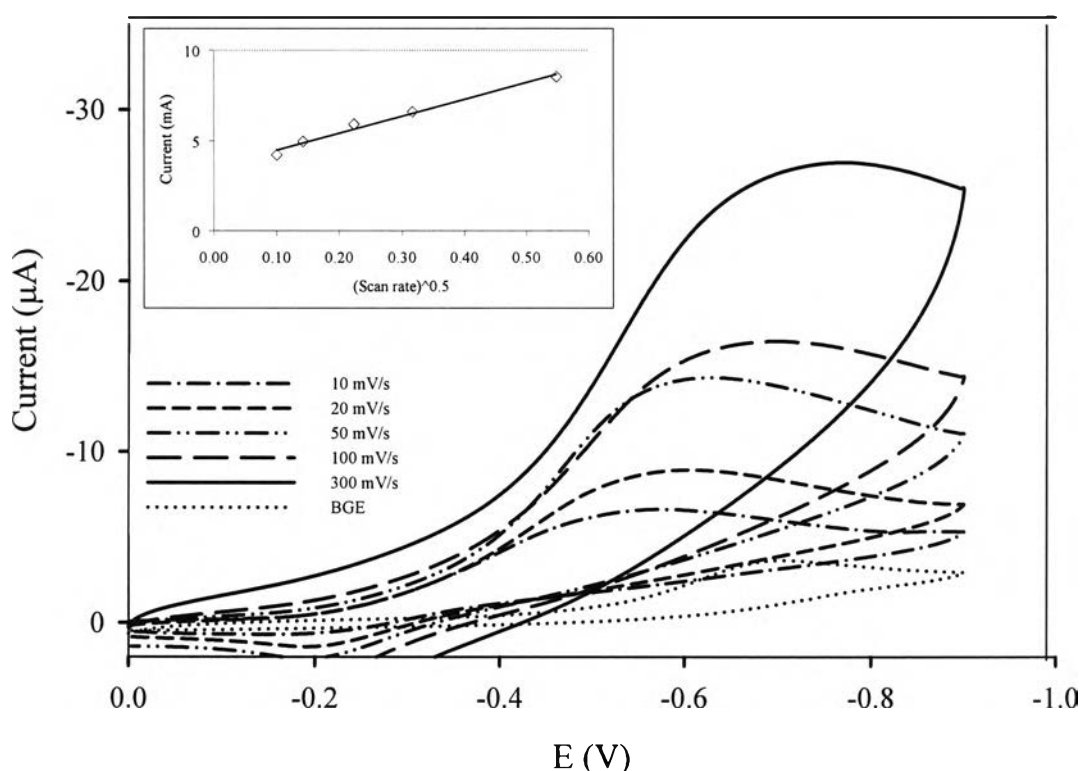
Figure 4.11 Cyclic voltammogram of 1 mM copper in 25 mM MES and L-histidine (pH 7.0) buffer at the screen-printed carbon electrode. The scan rate is 10-300 mV/s. The relationship of current signal and square root of scan rate is also shown in this Figure (inset).

## 4.2 Microchip for separation and detection of metal ions

Microchip capillary electrophoresis (CE) has been introduced as a tool for fast analysis in a small instrument. Instead of bringing samples to the laboratory, it is possible to perform the analysis on-site. The microchip CE systems that are commercially available have been developed primarily for use in the field of life sciences where high throughput is the main benefit and quantitation is of lower importance than identification. In this chapter, we focus on the determination of metal ions, lead(II), cadmium(II) and copper(II), in drinking water using microchip CE. The aim of this work is to establish the requirements for accurate quantitation and to evaluate microchip CE performance in the field of water analysis.

It is well known that carrier electrolytes with low-mobility coion are preferred for analysis of small ions. 2-(*N*-Morpholino)ethanesulfonic acid (MES) + histidine is a typical carrier electrolyte with a low-mobility coion used for the separation of small ions because both compounds have relatively low mobilities. Moreover, their pK_a values are almost identical, which make them an excellent buffer system. In general, the first step for using microchip CE for the determination of metal ions is the selection of the background electrolyte coion, and subsequently, the optimization of the resolution and the detection sensitivity of the system. Particularly, when electrochemical detection is used; the background electrolyte has a large effect on the signal sensitivity. To obtain a high signal-to-background ratio, the ionic conductivity of the background electrolyte coion, which is directly related to the electrophoretic mobility, should differ from the analyte as much as possible. In the following parts, the influence of some experimental parameters such as: the buffer pH, buffer concentration, the separation voltage, and the detection potential on the separation efficiency and detection sensitivity are reported in detail.

4.2.1 Electrochemical characteristics of metal ions: lead(II), cadmium(II) and copper(II) ions.

The preliminary study of electrochemical reduction of the metal ions: lead (II), cadmium (II), and copper (II), was performed using a screen-printed carbon electrode in the MES buffer solution (pH 7.0). Figures 4.4-4.6 display the typical voltammetric responses for 1 mM lead, cadmium and copper in buffer solution. An approximate, but well defined reduction (Ep = -0.7, -0.8, and -0.6 V) were observed for lead, cadmium and copper (II), respectively.

The electrochemical characteristics of these three metal ions in microchip capillary electrophoresis were studied with a screen-printed electrode with amperometric detection. Figure 4.12 shows the electropherogram of the three metal ions in running buffer solution. The results illustrate the separation and sensitivity for analysis of these metals, with retention times of Pb^{2+}, Cd^{2+} and Cu^{2+} are 95, 120 and 145 s, respectively.
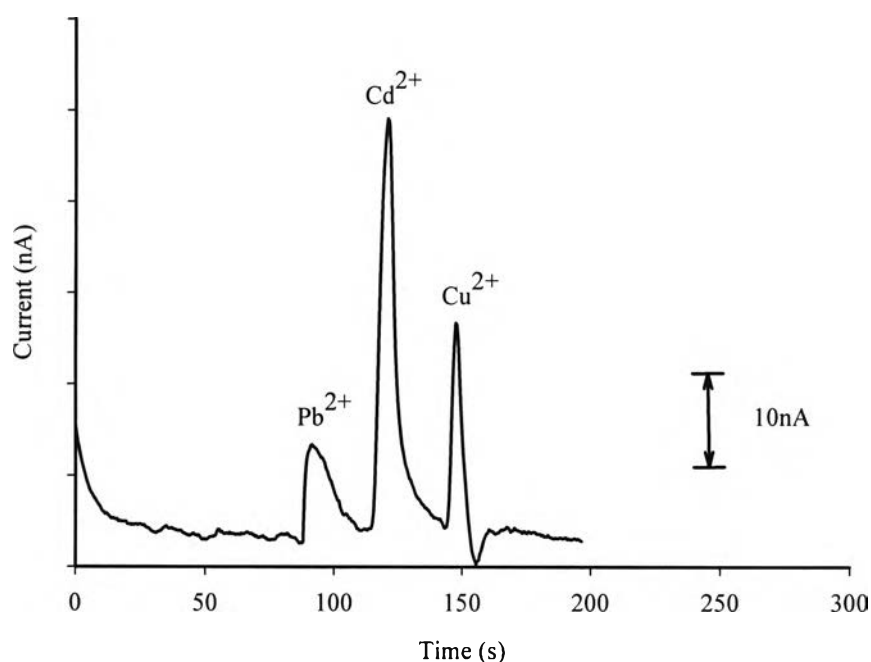
Figure 4.12 The electropherogram of metal ions: Pb^{2+}(a), Cd^{2+}(b), and Cu^{2+}(c). Experimental parameters: 1.0 mM mixed metal ions; running buffer, MES and L-histidine (pH 7.0); separation voltage 1100 V; detection

potential -0.8 V; sampling time 3 s; working electrode: screen-printed carbon electrode.

4.2.2 Influence of pH

The running buffer pH is the first important parameter for optimization in microchip CE; the same as in conventional CE, in which the separation medium pH influenced the ζ potential of the interior of the capillary. The running buffer pH has effect on the: EOF rate, ionization degree, mobility, and separation efficiency of the analytes. Thus, the pH values of running buffer were examined in the pH range of 6.0-8.5. All buffers contained 20 mM MES and 20 mM L-histidine. Therefore, we studied the effect of the buffer pH on the separation efficiency. Table 4.2 lists the effect of running buffer pH on the resolution (Rs) of Cd^{2+}, Pb^{2+} and Cd^{2+},Cu^{2+}. Rs gradually increases from 1.45 to 2.58 for Cd^{2+} and Pb^{2+}, and from 1.05 to 3.33 for Cd^{2+} and Cu^{2+} as the buffer pH decreases from 8.5 to 6.5. Further reducing the buffer pH causes the peak currents to decrease (data not shown).

Table 4.2 Current and Resolution of three metal ion standards in 20 mM MES containing 20 mM L-His; when 1.2 kV voltage; and -0.85 V detection voltage are applied.

| pH Of BGE	Current (nA)			Resolution	
	Pb(II)	Cd(II)	Cu(II)	$R_{Pb,Cd}$	$R_{Cd,Cu}$
6	7.35	7.35	1.87	-	7.75
6.5	1.98	14.81	7.88	2.58	2.51
7	13.49	25.71	17.09	1.91	3.33
7.5	13.25	18.48	10.99	2.18	2.31
8	14.69	20.42	13.69	1.45	1.18
8.5	11.38	11.89	10.35	1.79	1.05

This table clearly shows that selection of CE conditions hinges upon considering the two factors of separation efficiency and detection sensitivity. The results show the current and resolution of three metal ions. It can be seen that when the buffer pH was set between 6.5 and 7.5, the three metal ions could be well separated. The highest current signal was obtained at buffer pH 7.5. Higher buffer pH, not only increased the background noise signal but also took increasing time for stabilization of baseline. Therefore, a buffer pH 7.0 was selected as optimal for all subsequent work.

### 4.2.3 Influence of electrolyte concentration

Buffer concentration is another important parameter that hardly effect on the separation efficiency and detection sensitivity. Electropherograms of 1.0 mM lead, cadmium and copper in varying concentrations of pH 7.0 buffer were performed. It was found that the buffer concentration had negligible influence on the migration time of the analytes; and was found that the peak current of the three cations increased with increasing buffer concentrations from 10 to 25 mM, and then decreased with the further increase of the buffer concentration as shown in Figures 4.13-4.15. Generally, in order to minimize electromigrative dispersion, and to obtain high separation efficiencies, the mobilities of analyte ions and carrier electrolyte coion should be similar. For carrier electrolytes with low-mobility coion, such as MES + histidine, high concentrations make for electrostacking, which helps to suppress peak dispersion.
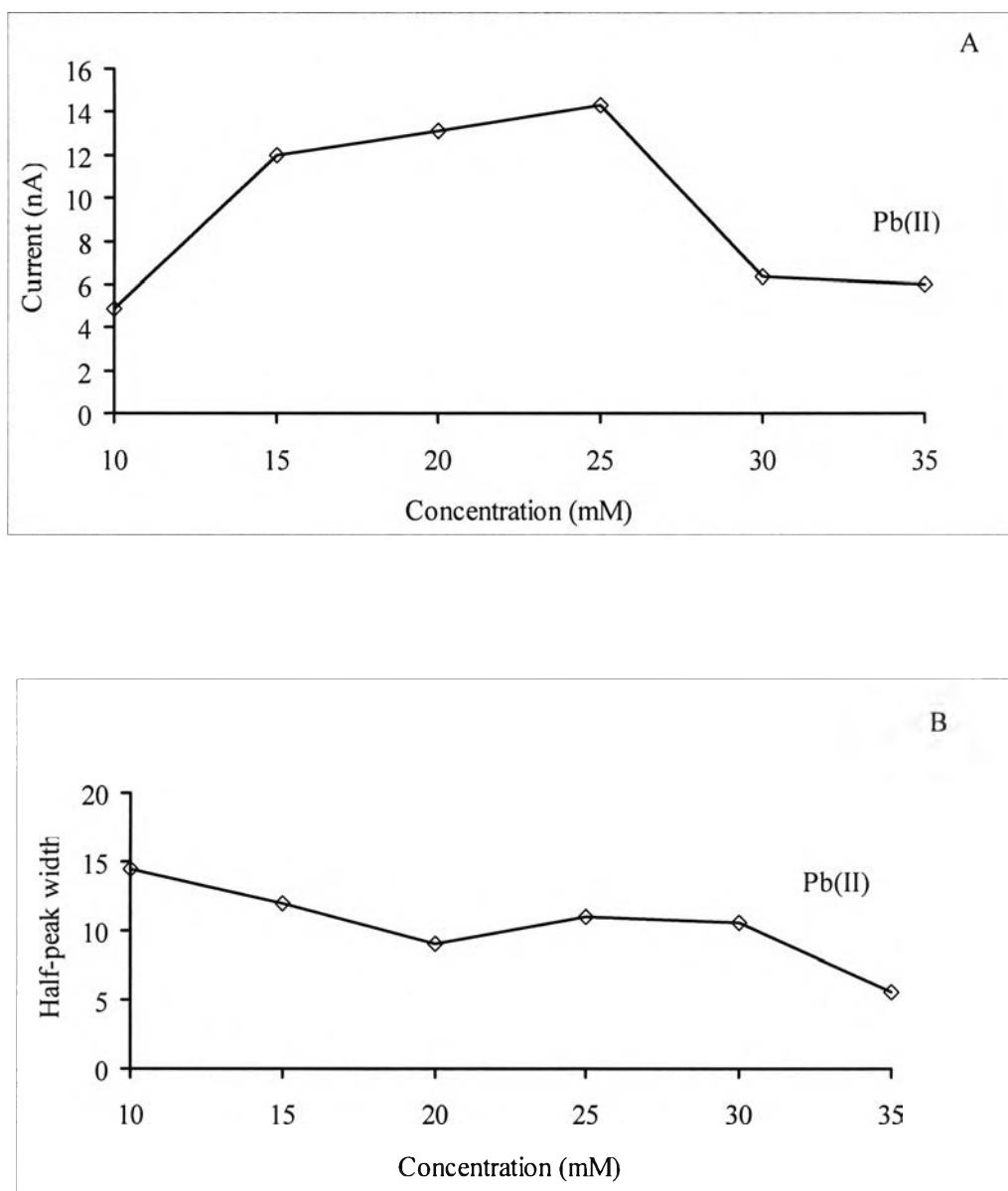
Figure 4.13 The effects of the buffer concentration on: (A) peak current, and (B) half-peak widths of 1.0 mM lead(II) ion. Experimental parameters :   running buffer, MES and L-His pH 7.0; separation voltage 1000 V; detection potential -0.8 V; sampling time 3 s; screen-printed carbon electrode.
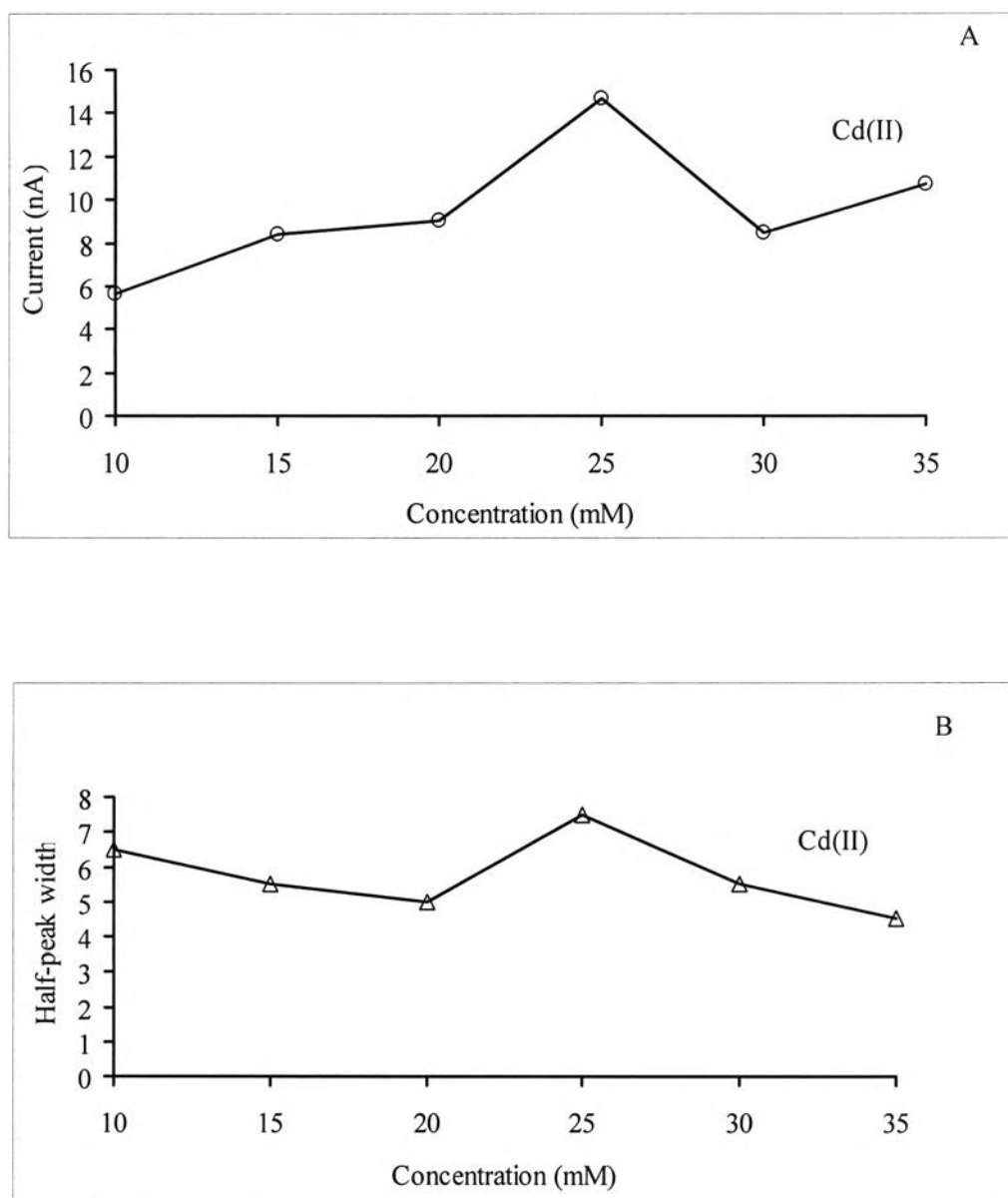
Figure 4.14 The effect of the buffer concentration on: (A) peak currents, and (B) half-peak widths of 1.0 mM cadmium(II) ion. Experimental parameters : running buffer, MES and L-His pH 7.0; separation voltage 1000 V; detection potential -0.8 V; sampling time 3 s; working electrode, screen-printed carbon electrode.
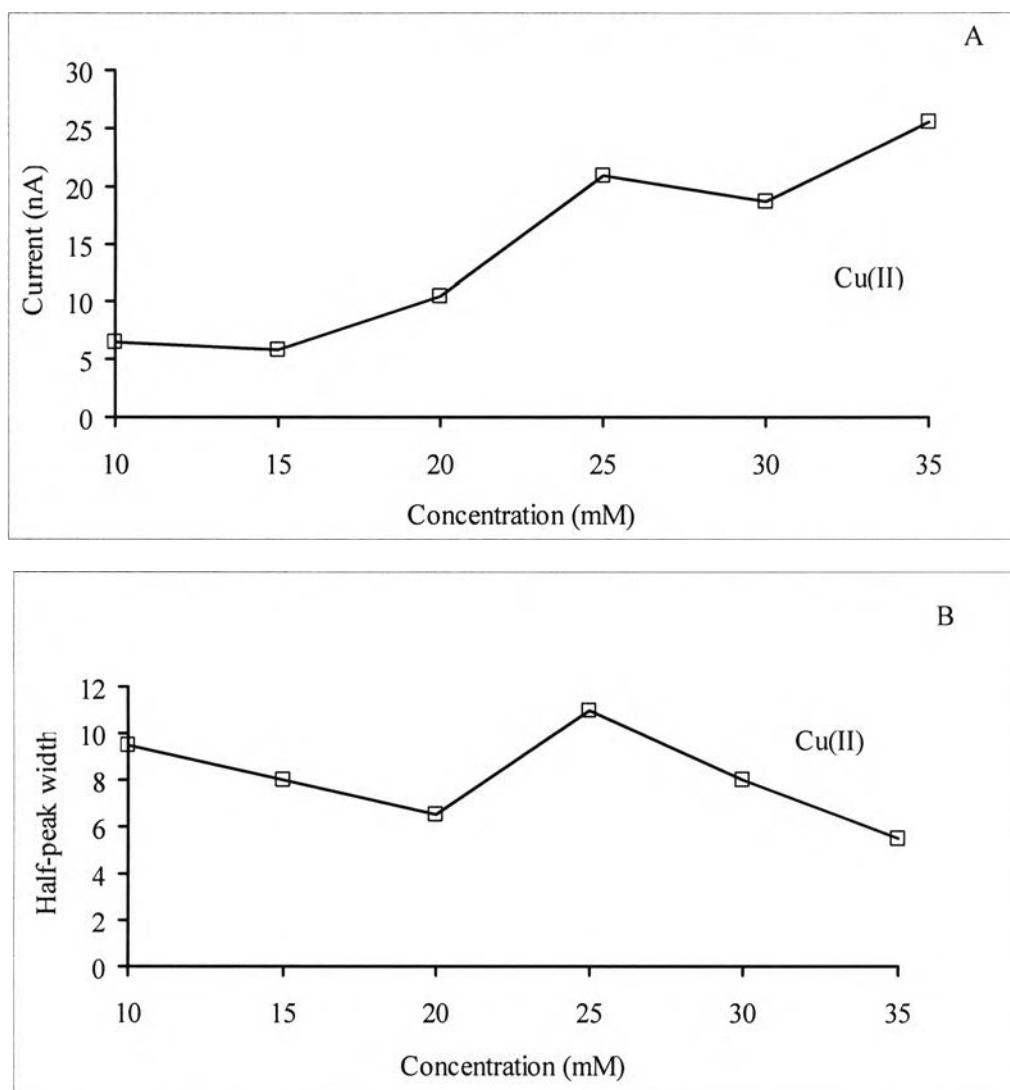
Figure 4.15 The effects of the buffer concentration on: (A) peak currents, and (B) half-peak widths of 1.0 mM copper(II) ion. Experimental parameters: running buffer, MES and L-His pH 7.0; separation voltage 1000 V; detection potential -0.8 V; sampling time 3 s; working electrode: screen-printed carbon electrode.

This phenomenon can occur for two reasons: (1) higher concentration of running buffer will result in higher ionic strength, which will decrease the conductivity difference between the sample and running buffer, and result in low signal, and (2), the higher concentration of the running buffer used for electrostacking, which results in relatively higher concentrations of the sample zone and then a relatively high signal is obtained. In relation to the factor of detection sensitivity, the running buffer concentration of 25 mM was chosen.

4.2.4 Influence of detection potential

The detection potential strongly affects the sensitivity and detection limits of microchip CE with an electrochemical detection system. In order to obtain the optimal detection potential, a hydrodynamic voltammogram was investigated. Figure 4.16 shows a compromise between low applied potentials and enough sensitivity for all the metal ions involved at the screen-printed carbon electrode. The influence of the detection potential applied to the working electrode was studied for Pb^{2+}, Cd^{2+} and Cu^{2+}.
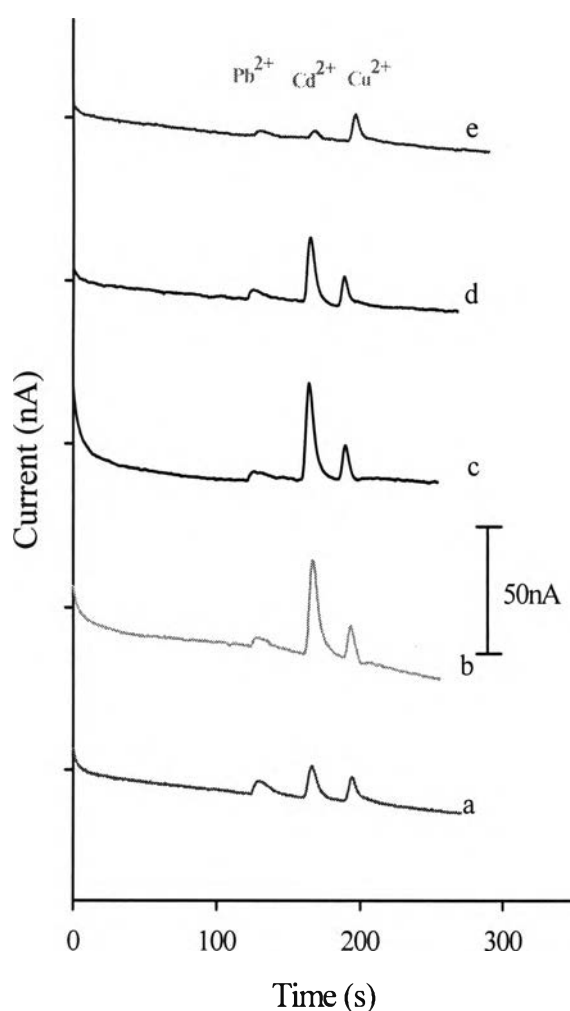
Figure 4.16 Electropherograms of 1.0 mM lead, cadmium and copper cations at different detection potentials, -0.90 V (a), -0.85 V (b), -0.80 V (c), -0.75 V (d), -0.70 V (e). Experimental parameters : 25 mM MES and L-His pH 7.0 used as running buffer; separation voltage 1000 V; sampling time 3 s.
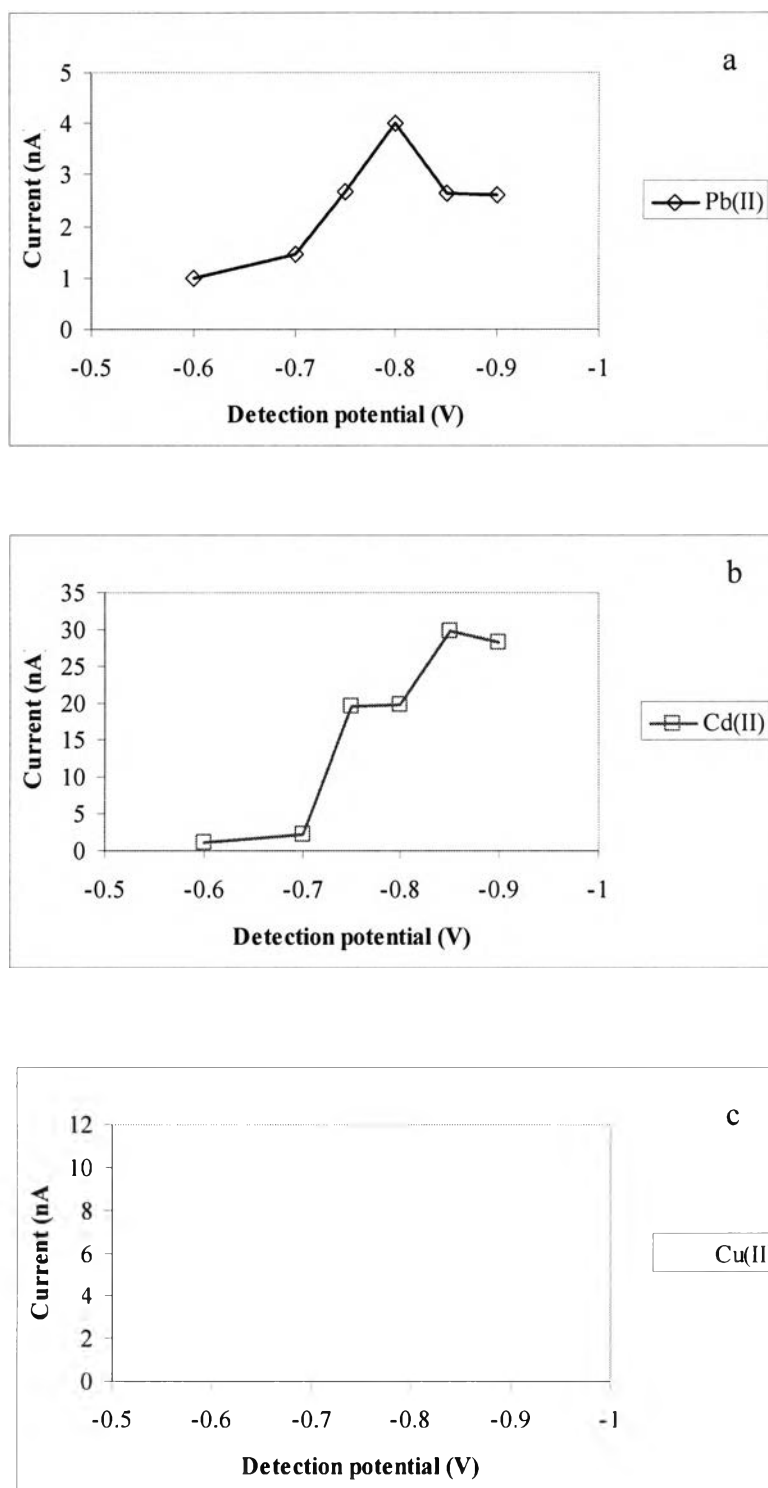
Figure 4.17 The relationship between the peak current and the separation voltage of 1.0 mM copper(II) ion at different detection potentials when tested against: Pb(II) (a), Cd(II) (b), Cu(II) (c). Experimental parameters : 25 mM MES and L-His pH 7.0 used as running buffer; separation voltage 1000 V; sampling time 3 s; working electrode, screen-printed carbon electrode.

It was observed that the amperometric signal of these heavy metals ions increased with increasing detection potential from -0.70 to -0.85 V. However, the baseline current and the corresponding noise level become large at lower reduction potentials. The sensitivity of the signal for the three ions changes with changing detection potentials as shown in Figure 4.17. From the results, it can be seen that cadmium and copper have similar changes in signal rates, while the relative peak current of lead has a lower change rate with the changing detection potential. To compensate between the sensitivity and signal-to-noise characteristics for simultaneous metals analysis, a detection potential of -0.8 V offered the most favorable result.

### 4.2.5 Influence of separation voltage

The separation voltage affects the electric field strength, which in turn affects the EOF and the migration velocity of charged particles, ultimately determining the migration time of analytes. Since the electrochemical detection principle is based on the coupling of the separation electric field to the electrochemical detector, the influence of separation voltage on detection is a major factor in improving detection sensitivity. Moreover, a higher separation voltage may result in higher Joule heating. The relationship between the amperometric response with different separation voltages are shown in Figure 4.18-4.20 for lead, cadmium, and copper cations, respectively.
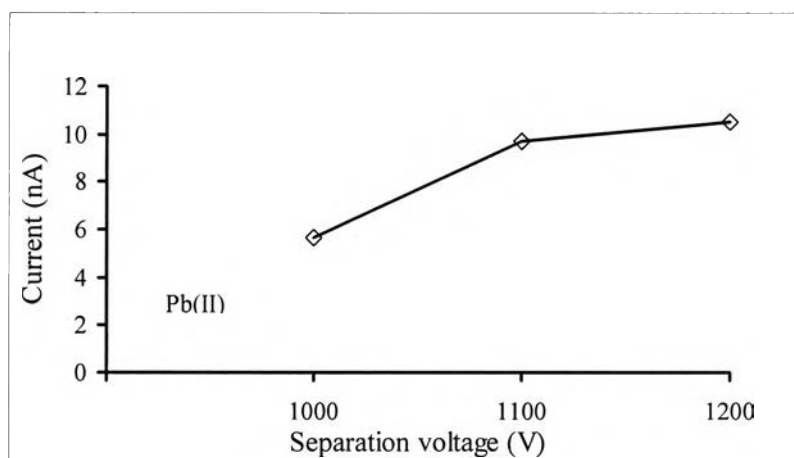
Figure 4.18 The relationship between the peak currents and the separation voltage. The amperometric response of 1.0 mM lead(II) cations at different separation voltages. Other parameters are the same as in Figure 4.17.
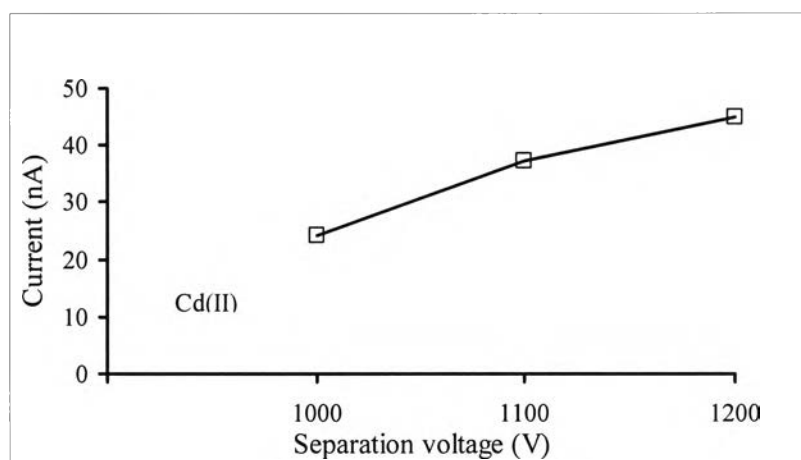
Figure 4.19 The relationship between the peak current and the separation voltage. The amperometric response of 1.0 mM cadmium(II) cations at different separation voltages. Other parameters are the same as in Figure 4.17.
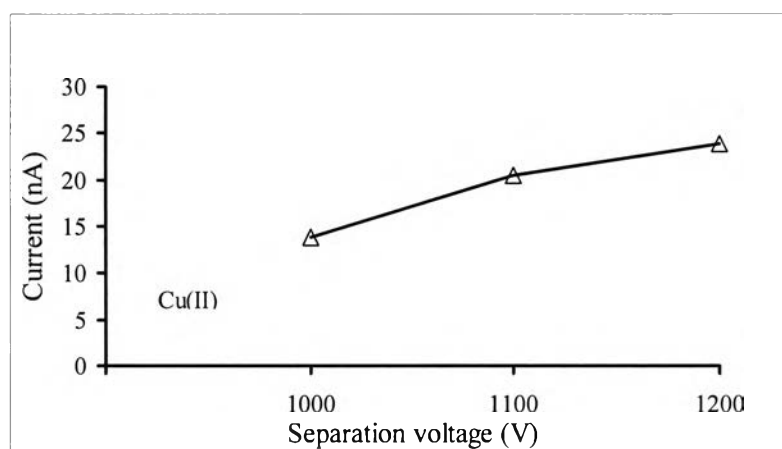
Figure 4.20 The relationship between the peak currents and the separation voltage. The amperometric response of 1.0 mM copper(II) cations at different separation voltages. Other parameters are the same as in Figure 4.17.

The effect of separation voltage on the migration time of the analytes is shown in Figure 4.21. By enhancing the separation voltage, the migration times of the three cations were clearly shorter due to the EOF and electrophoretic flow in same direction, which simultaneously increase with the increase of separation electric field.
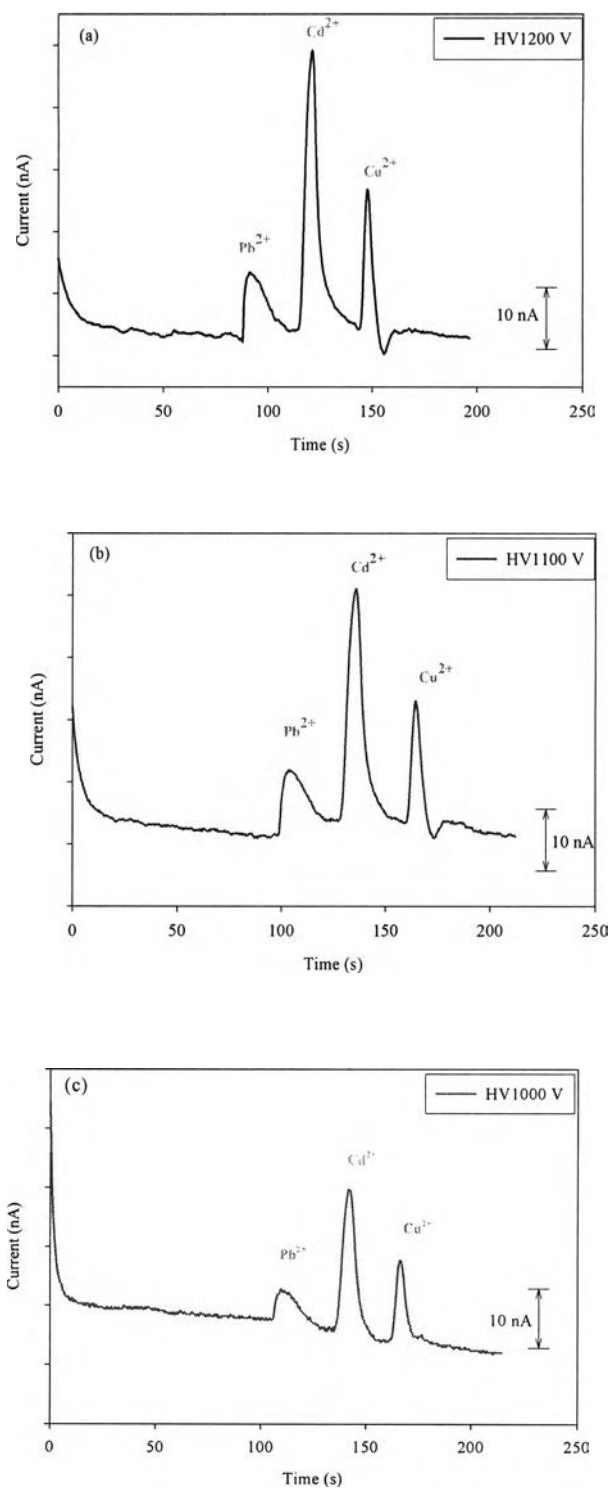
Figure 4.21 Electropherograms of 1.0 mM lead, cadmium and copper cations at different separation voltages. The relationship between the peak currents and the separation time: 1200 V (a), 1100 V (b), 1000 V (c). Other parameters are the same as in Figure 4.17.

In addition, a relative ascent of the amperometric signal was observed with the increasing voltage. The coupling effect on amperometric detection potential is stronger with increasing electric field separation, which were observed the larger peak currents corresponding to an accelerated electrochemical response. The sensitivity of the signal with the change in separation voltage is different for the three cations. As expected, increasing the voltage gives shorter migration times, but also increases the background noise, resulting in a higher detection limit. The migration times were dramatically decreased for all three metal ions: from 120 to 90 s for lead, 150 to 110 s for cadmium, and 175 to 140 s for copper. Although the resolution of analytes can be improved to some extent, too low a separation voltage will increase the analytical time considerably, which in turn causes severe peak broadening (Figure 4.21b). When the separation voltage was higher than 1200V, the baseline became more and more unsteady. It was suggested that a high separation voltage could produce an air bubble and consequently result in clogging of the channel. Based on these experiments, 1200 V was chosen as the optimum voltage to accomplish optimal results.

4.2.6 Linear range and detection limit

According to previous studies on the running buffer pH and concentration, as well as separation voltage and detection potential, the optimized conditions of 1200 V separation voltage, -0.8 V detection potential, and 25 mM (pH 7.0) MES + L-His as running buffer were obtained. Under the selected conditions, a series of standard mixture solutions containing lead, cadmium, and copper with concentrations ranging from 100 μM to 1000 μM were tested to determine the linearity for all analytes at the screen-printed carbon electrode in this system as shown in Figures 4.22-4.24 for Pb^{2+}, Cd^{2+}, and Cu^{2+}, respectively.
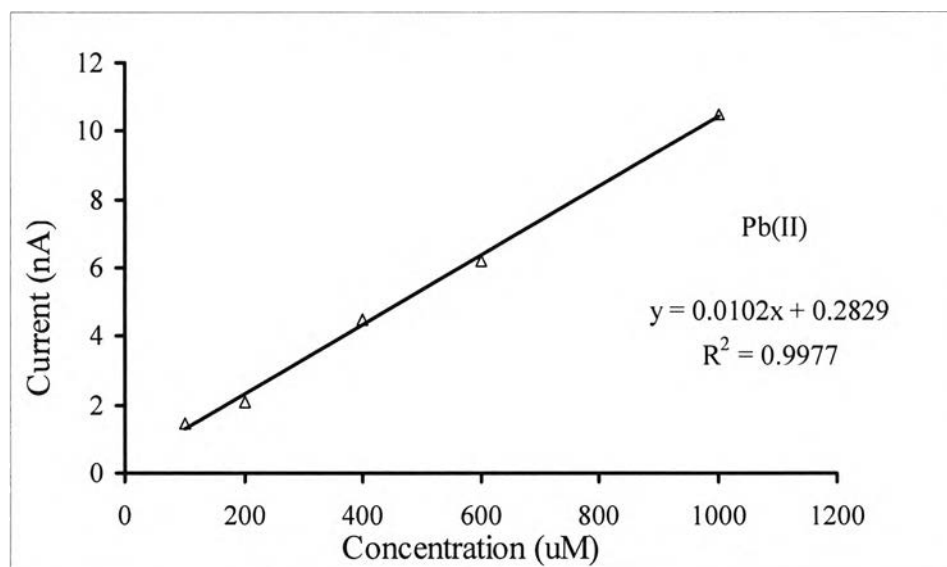
Figure 4.22 The relationship between the peak currents and the concentration of lead(II) ion. Experimental parameters: 25 mM MES and L-His pH 7.0 used as running buffer; separation voltage, 1200 V; detection potential, -0.8 V; sampling time 3 s; working electrode, screen-printed carbon electrode.
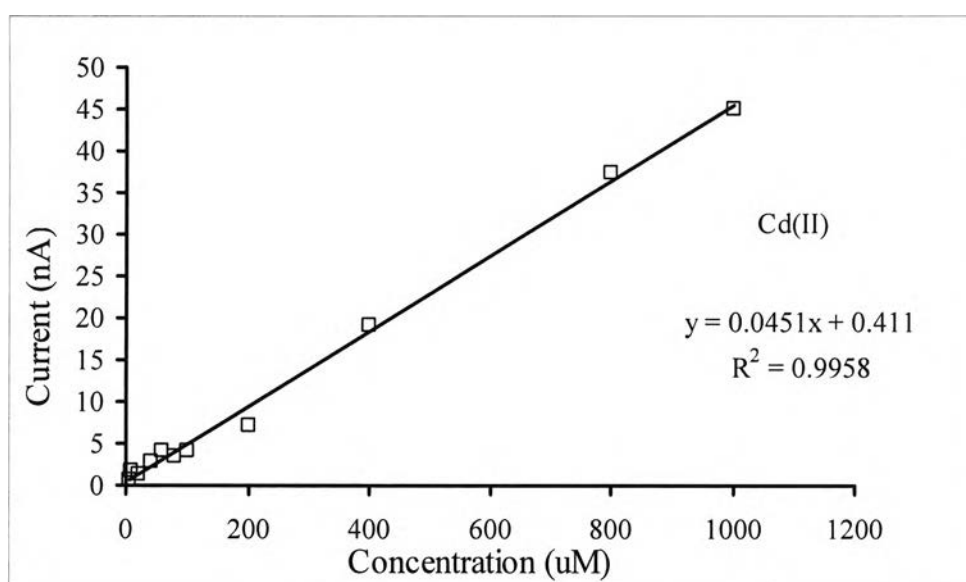
Figure 4.23 The relationship between the peak currents and the concentration of cadmium(II) ion. Experimental parameters: 25 mM MES and L-His pH 7.0 used as running buffer; separation voltage, 1200 V; detection potential, -0.8 V; sampling time, 3 s; working electrode, screen-printed carbon electrode.
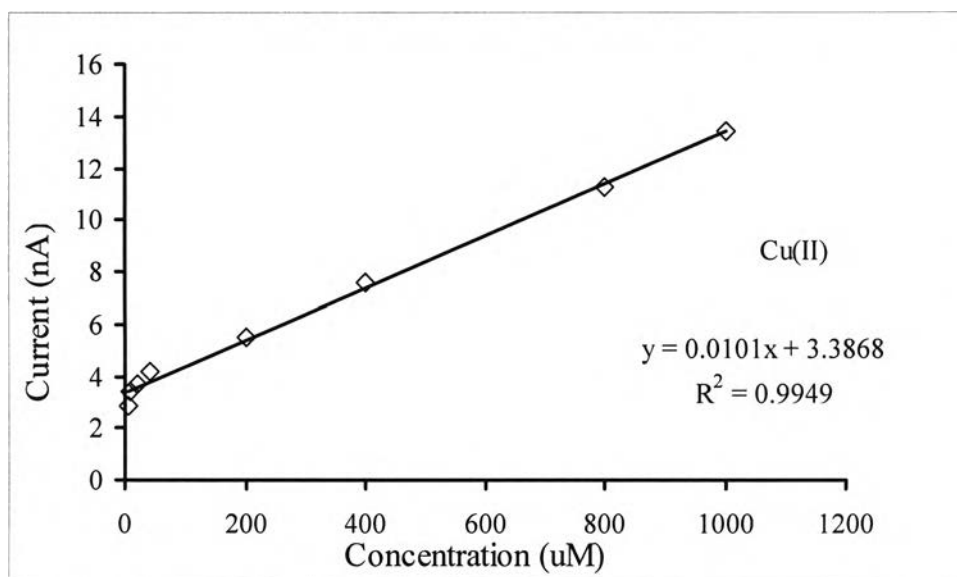
Figure 4.24 The relationship between the peak currents and the concentration of copper(II) ion. Experimental parameters: 25 mM MES and L-His pH 7.0 used as running buffer; separation voltage, 1200 V; detection potential, -0.8 V; sampling time, 3 s; working electrode, screen-printed carbon electrode.

The results of regression analyses on the calibration curves are: 0.9977, 0.9958, and 0.9949 for lead, cadmium, and copper. The detection limits were evaluated on the basis of a signal-to-noise ratio of 3. The calibration curves exhibit excellent linear behavior over the concentration range of about micromolar orders of magnitude with the detection limits ranging from 0.13 to 1.74 μM for all the metal ions.

4.2.7 Repeatability and Accuracy

A standard mixture solution of lead, cadmium, and copper (1 mM each) was analyzed ten times to determine the reproducibility of the peak current and migration time for all analytes under the optimum conditions in this experiment. These optimized conditions are: 1200 V separation voltage, −0.8 V detection potential, 25 mM (pH 7.0) of MES + L-His as running buffer, and injection time 3 s. The average peak current, SD and %RSD of the three metal ion signals are shown in Table 4.3. The reproducibility of retention times and half-width peaks in the analysis of Cu^{2+}, Cd^{2+} and Pb^{2+} are shown in Table 4.4 and Table 4.5, respectively.

Table 4.3 The reproducibility of peak current for the detection of metals. Other parameters are the same as in Figure 4.22

Metals	Peak current (average)	SD	%RSD
Pb(II)	9.28	0.39	4.20
Cd(II)	26.23	1.38	5.27
Cu(II)	13.15	0.52	3.92

Table 4.4 The reproducibility of half-width peak for the detection of metals. Other parameters are the same as in Figure 4.22

Metals	Half-width Peak (average)	SD	%RSD
Pb(II)	9.92	0.79	7.97
Cd(II)	5.17	0.46	8.98
Cu(II)	4.50	0.35	7.86

Table 4.5 The reproducibility of retention times for the detection of metals. Other parameters are the same as in Figure 4.22

Metals	Retention time (average)	SD	%RSD
Pb(II)	91.5	1.36	1.47
Cd(II)	116.5	1.66	1.40
Cu(II)	140.0	1.71	1.20

The relative standard deviations (RSDs) of peak currents and migration times are: 4.20 % and 1.47 % for lead, 5.27 % and 1.40 % for cadmium, 3.92 % and 1.20 % for copper, respectively. It is indicated that the proposed system exhibited an excellent performance in both separation and detection for prolonged operation.

### 4.2.8 Real sample analysis

Metal ions are essential components of biological systems; however, they may have toxic or carcinogenic properties at high concentrations. The contamination of our environment (such as water and soil) due to heavy metal ions is a very serious and challenging problem. Therefore, it is very important to analyze the presence of heavy metal ions in the environment. Under optimum conditions, the determination of lead, cadmium, and copper in real samples was carried out according to the procedures described earlier.

4.2.8.1 Analysis of metal ions in Unif's green vegetable juice

Microchip CE with amperometric detection system was applied to the determination of analytes in the beverage, Unif's green vegetable juice. The standard addition method was used to determine the amount of metal ions in theses samples.

4.2.8.1.1 Analysis of lead(II) ion in a Unif's green vegetable juice

The determination of lead(II) ion in a Unif's green vegetable juice when using the screen-printed carbon electrode in the microchip CE system is displayed in Figure 4.27. From these results, the relationship between the current response and the concentration of analyte under the selected condition is apparent. A series of standard solutions with a concentration range of 0 μM to 1000 μM was used to determine the linearity of analysis. The results of regression analysis are 0.9950. Table 4.6 lists the obtained %recovery, SD, and %RSD from the analysis of Pb^{2+} ion in these samples.
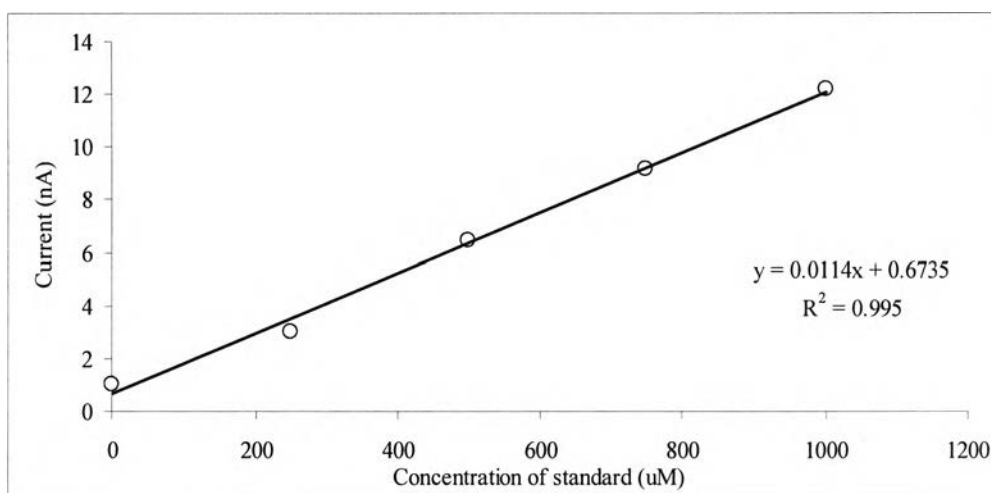
Figure 4.25 The relationship between the peak currents and the concentration of lead(II) ion in Unif's green vegetable juice. Experimental parameters: 25 mM MES and L-His pH 7.0 used as running buffer; separation voltage, 1200 V; detection potential, -0.8 V; sampling time, 3 s; working electrode, screen-printed carbon electrode.

Table 4.6 The %recovery of analysis of lead(II) ion in Unif's green vegetable juice. Other parameters are the same as in Figure 4.25.

Concentration (μM)	%recovery					
	Pb(II) ion					
	1	2	3	average	SD	%RSD
1000	101.71	101.20	106.68	103.20	3.03	2.93
750	100.14	99.26	103.77	101.06	2.39	2.37
500	94.45	100.97	96.76	97.39	3.31	3.40
250	81.76	82.33	90.63	84.91	4.96	5.85

4.2.8.1.2 Analysis of cadmium(II) ion in Unif's green vegetable juice

The microchip CE with amperometric detection system was used for determination of cadmium(II) ion in Unif's green vegetable juice when using the screen-printed carbon electrode is displayed in Figure 4.26. From these results, the relationship between the current response and the concentration of analyte under the optimum condition is apparent. A series of the standard solutions with a concentration range of 0 μM to 1000 μM was used to determine the linearity of analysis. The results of regression analysis are 0.9968. Table 4.7 lists the %recovery, SD, and %RSD of analysis of Cd^{2+} ion in theses samples by standard addition method.
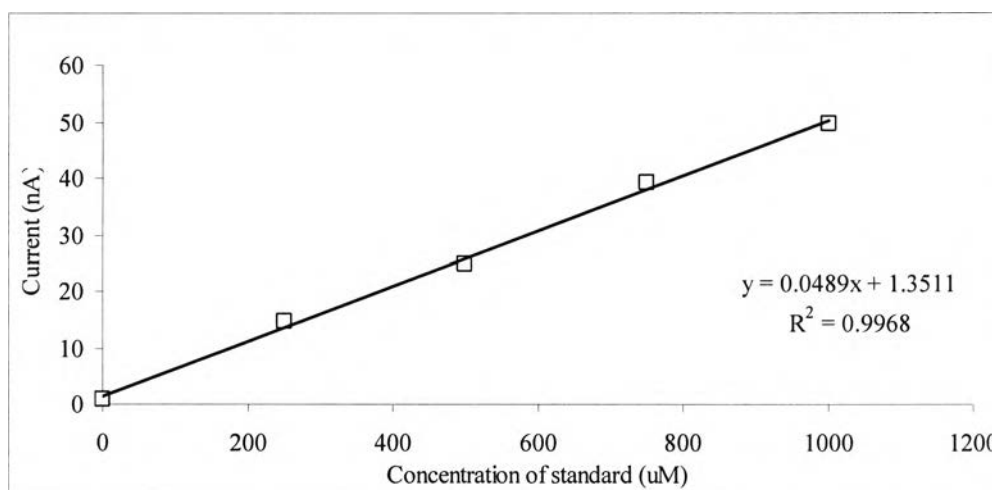

$$y = 0.0489x + 1.3511$$
$$R^2 = 0.9968$$

Figure 4.26 The relationship between the peak currents and the concentration of lead(II) ion in Unif's green vegetable juice. Experimental parameters: 25 mM MES and L-His pH 7.0 used as running buffer; separation voltage 1200 V; detection potential, -0.8 V; sampling time, 3 s.

Table 4.7 The %recovery of analysis of cadmium(II) ion in Unif's green vegetable juice. Other parameters are the same as in Figure 4.26.

Concentration (µM)	%recovery					
	Cd(II) ion					
	1	2	3	average	SD	%RSD
1000	98.67	96.73	97.11	97.50	1.03	1.05
750	103.36	105.58	107.80	105.58	2.22	2.10
500	95.46	97.69	93.13	95.43	2.28	2.39
250	109.03	109.41	105.26	107.90	2.30	2.13

4.2.8.1.3 Analysis of copper(II) ion in Unif's green vegetable juice

The determination of copper(II) ion in Unif's green vegetable juice when using the screen-printed carbon electrode in microchip CE system was observed in Figure 4.27. From these results, there is a clear relationship between the current response and the concentration of analyte under the MES and L-histidine running buffer solution. A series of standard solutions with a concentration range of 0 to 1000 µM was used to determine the linearity of analysis. The results of regression analysis are 0.9956. Table 4.8 shows the %recovery, SD and %RSD from analysis of Cu^{2+} ion in theses samples by standard addition method.

$$y = 0.0215x + 0.4247$$
$$R^2 = 0.9956$$

Figure 4.27 The relationship between the peak currents and the concentration of lead(II) ion in Unif's green vegetable juice. Experimental parameters: 25 mM MES and L-His pH 7.0 used as running buffer; separation voltage, 1200 V; detection potential, -0.8 V; sampling time 3 s.
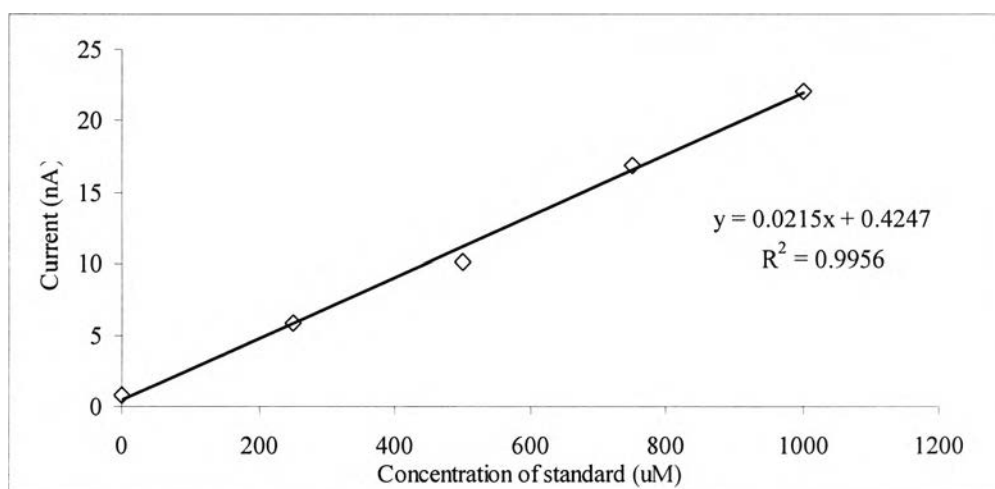
Table 4.8 The %recovery from analysis of copper(II) ion in Unif's green vegetable juice. Other parameters are the same as in Figure 4.27.

Concentration (μM)	%recovery					
	Cu(II) ion					
	1	2	3	average	SD	%RSD
1000	100.91	97.74	99.00	99.22	1.59	1.61
750	102.05	105.58	106.11	104.58	2.21	2.11
500	90.75	94.75	90.28	91.93	2.46	2.67
250	101.49	102.82	95.77	100.03	3.75	3.75

4.2.8.2 Analysis of metal ions in Malee's tomato juice

Microchip CE with an amperometric detection system was applied to the determination of the beverage, Malee's tomato juice. The standard addition method was used to determine the amount of metal ions in these samples.

4.2.8.2.1 Analysis of lead(II) ion in Malee's tomato juice

Figure 4.28 shows the results for determination of lead(II) ion in Malee's tomato juice when using the screen-printed carbon electrode in a microchip CE system. From the results, the relationship between the current response and the concentration of analyte under the optimum condition is apparent. A series of standard solutions with a concentration range of 0 μM to 600 μM was used to determine the linearity of the analysis system. The results of regression analysis are 0.9952. The %recovery, SD and %RSD of analysis of Pb^{2+} ion are listed in Table 4.9.
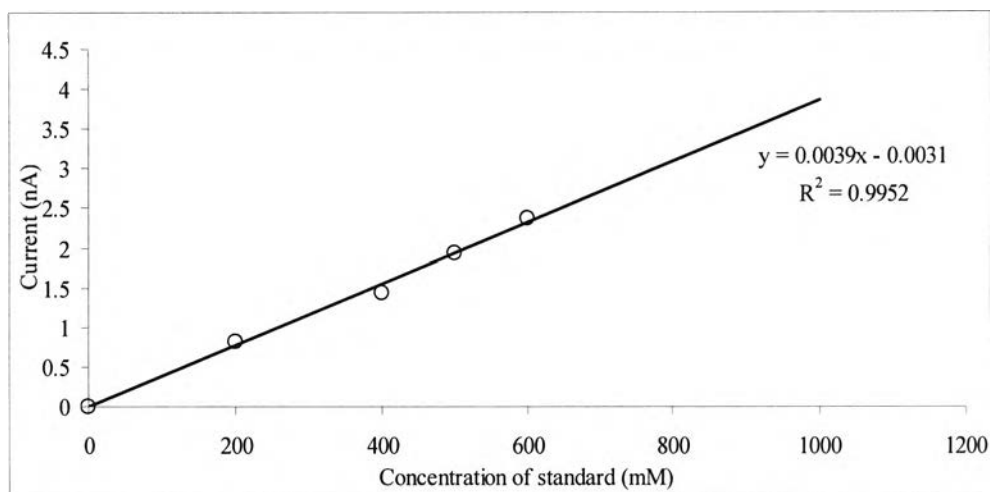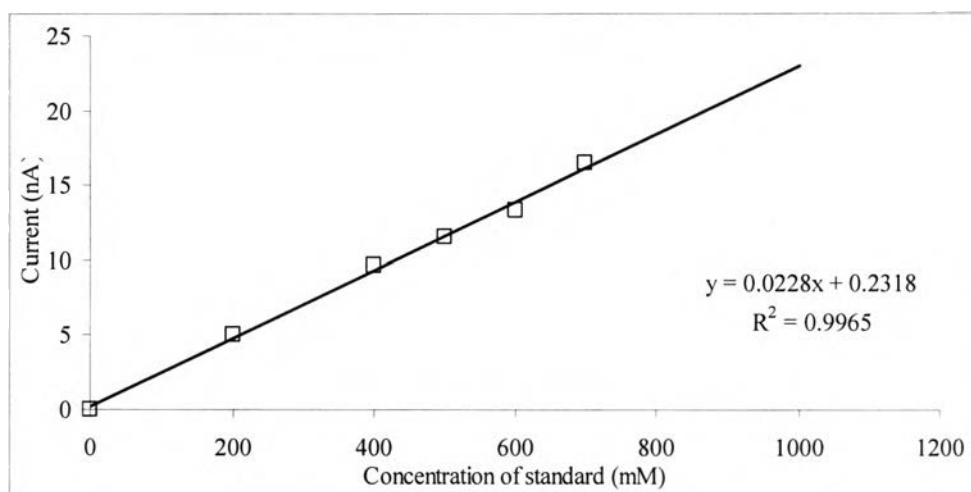
Figure 4.28 The relationship between the peak current and the concentration of lead(II) ion in Malee's tomato juice. Experimental parameters: separation voltage, 1200 V; detection potential, -0.8 V; sampling time 3 s; working electrode, screen-printed carbon electrode.

Table 4.9 The %recovery from analysis of lead(II) ion in Malee's tomato juice. Other parameters are the same as in Figure 4.28

Concentration (µM)	%recovery Pb(II) ion					
	1	2	3	average	SD	%RSD
1000	98.56	103.93	101.35	101.28	2.69	2.65
800	103.11	94.71	98.86	98.89	4.20	4.25
600	91.52	96.16	92.16	93.28	2.52	2.70
400	101.99	92.73	105.22	99.98	6.48	6.48

4.2.8.2.2 Analysis of cadmium(II) ion in Malee's tomato juice

The determination of cadmium (II) ion in Malee's tomato juice when using the screen-printed carbon electrode in microchip CE system is illustrated in Figure 4.29. From these results, the relationship between the current response and the concentration of analyte under the MES and L-histidine running buffer solution is apparent. A series of the standard solutions with a concentration range of 0 µM to 800 µM was used to determine the linearity of the analysis. The results of regression analysis are 0.9965. Table 4.10 showed the %recovery, SD and %RSD of analysis of Cd^{2+} ion in these samples.
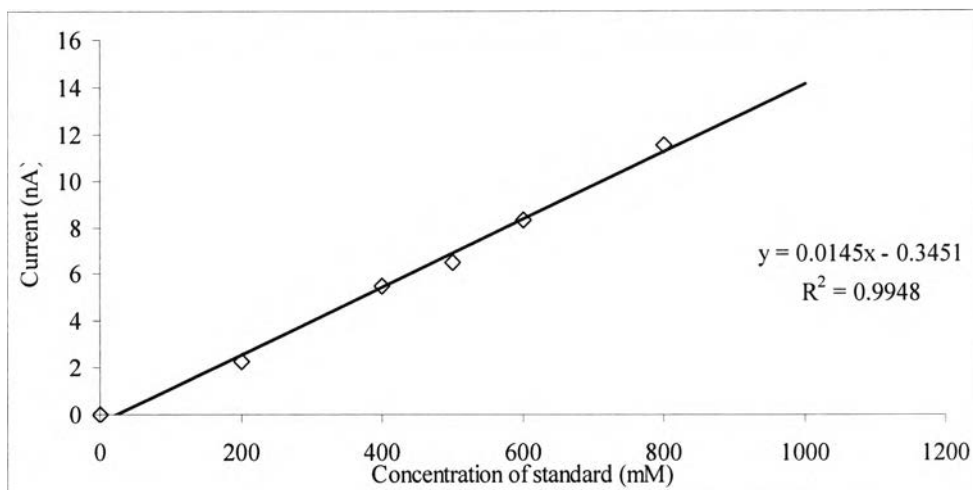
Figure 4.29 The relationship between the peak currents and the concentration of cadmium(II) ion in Malee's tomato juice. Experimental parameters: 25 mM MES and L-His pH 7.0 used as running buffer; separation voltage, 1200 V; detection potential, -0.8 V; sampling time, 3 s.

Table 4.10 The %recovery from analysis of cadmium (II) ion in Malee's tomato juice. Other parameters are the same as in Figure 4.29

Concentration (μM)	%recovery					
	Cd(II) ion					
	1	2	3	average	SD	%RSD
1000	102.90	98.14	101.73	100.92	2.48	2.46
800	97.01	97.77	96.02	96.93	0.88	0.90
600	102.24	100.30	98.99	100.51	1.63	1.63
400	107.70	107.76	103.46	106.31	2.47	2.32
200	100.41	94.09	106.26	100.25	6.09	6.07

4.2.8.2.3 Analysis of copper(II) ion in Malee's tomato juice

The determination of copper(II) ion in Malee's tomato juice when using the screen-printed carbon electrode in the microchip CE system is displayed in Figure 4.30. From these results, the relationship between the current response and the concentration of analyte under the selected condition is evident. A series of standard solutions with a concentration range of 0 μM to 800 μM was used to determine the linearity of the analysis. The result of regression analysis is 0.9948. Table 4.11 shows the %recovery, SD and %RSD for analysis of Cu^{2+} ion in these samples.

Figure 4.30 The relationship between the peak currents and the concentration of copper(II) ion in Malee's tomato juice. Experimental parameters: 25 mM MES and L-His pH 7.0 used as running buffer; separation voltage, 1200 V; detection potential, -0.8 V; sampling time, 3 s.

Table 4.11 The %recovery from analysis of copper(II) ion in Malee's tomato juice. Other parameters are the same as in Figure 4.30

Concentration (µM)	%recovery					
	Cu(II) ion					
	1	2	3	average	SD	%RSD
1000	102.64	101.15	102.63	102.14	0.86	0.84
800	94.74	98.88	99.59	97.73	2.62	2.68
600	91.42	93.42	94.96	93.26	1.78	1.90
400	92.24	99.01	101.11	97.45	4.64	4.76
200	101.97	94.58	90.20	95.59	5.95	6.23

4.2.8.3 Analysis of metal ions in Malee's pineapple juice

Microchip CE with the amperometric detection system was applied to the determination of analyte concentrations in the beverage, Malee's pineapple juice. Standard addition was used to determine the amount of metal ions in these samples.

4.2.8.3.1 Analysis of lead(II) ion in Malee's pineapple juice

The microchip CE with amperometric detection system was used to determine the amount of cadmium(II) ion in Malee's pineapple juice by using the screen-printed carbon electrode (Figure 4.31). From these results, the relationship between the current response and the concentration of analyte under optimum conditions was apparent. A series of standard solutions with a concentration range of 0 µM to 800 µM was used to determine the linearity of analysis. The results of regression analysis are 0.9966. Table 4.12 show the obtained %recovery, SD and %RSD of analysis of Pb^{2+} ion in theses samples.

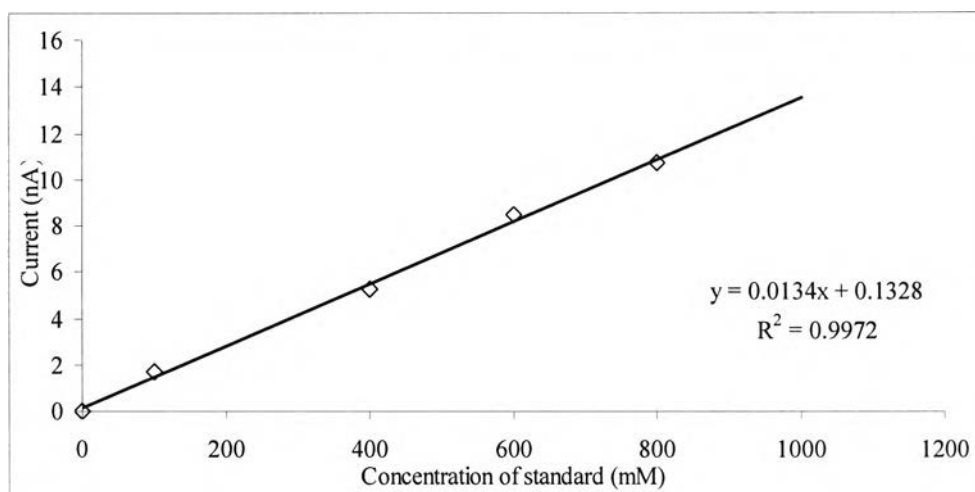$y = 0.0049x + 0.048$
$R^2 = 0.9966$
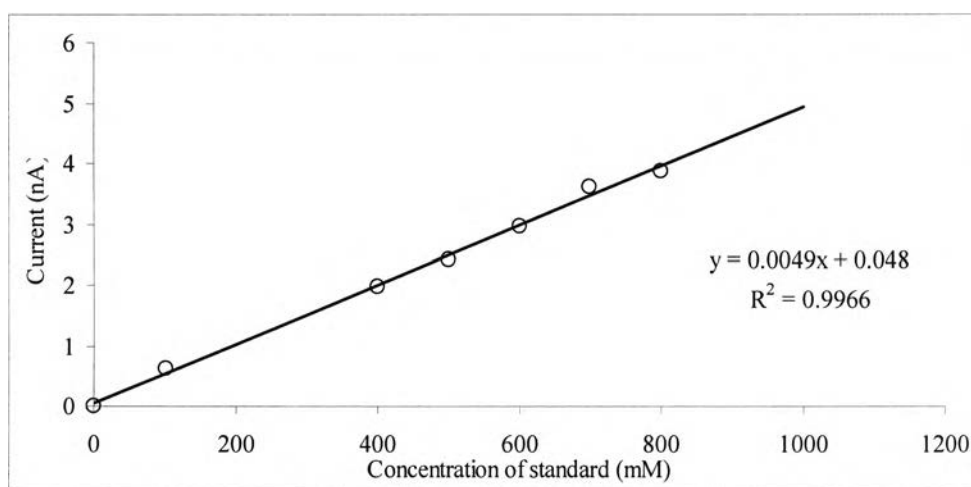
Figure 4.31 The relationship between the peak currents and the concentration of lead(II) ion in Malee's pineapple juice. Experimental parameters: 25 mM MES and L-His pH 7.0 used as running buffer; separation voltage, 1200 V; detection potential, -0.8 V; sampling time, 3 s; working electrode, screen-printed carbon electrode.

Table 4.12 The %recovery of analysis of lead(II) ion in Malee's pineapple juice. Other parameters are the same as in Figure 4.31.

Concentration (μM)	%recovery					
	Pb(II) ion					
	1	2	3	average	SD	%RSD
800	105.05	98.23	103.89	102.39	3.65	3.56
700	100.93	104.68	102.80	102.80	1.87	1.82
600	96.80	99.48	96.85	97.71	1.53	1.57
500	96.03	96.46	94.53	95.67	1.02	1.06
400	101.57	98.03	97.82	99.14	2.11	2.13
100	105.59	106.30	101.10	104.33	2.82	2.70

4.2.8.3.2 Analysis of cadmium(II) ion in Malee's pineapple juice

The analysis of cadmium(II) ion in Malee's pineapple juice with microchip CE with amperometric detection system using the screen-printed carbon electrode is shown in Figure 4.32. From these results, the relationship between the current response and the concentration of analyte under the optimum conditions is evident. A series of standard solutions with a concentration range of 0 μM to 800 μM was used to determine the linearity of analysis. The results of regression analysis are 0.9972. The %recovery, SD and %RSD of analysis of Cd^{2+} ion in theses samples is shown in Table 4.13.

Figure 4.32 The relationship between the peak currents and the concentration of cadmium(II) ion in Malee's pineapple juice. Experimental parameters: 25 mM MES and L-His pH 7.0 used as running buffer; separation voltage, 1200 V; detection potential, -0.8 V; sampling time, 3 s; working electrode, screen-printed carbon electrode.

Table 4.13 The %recovery from analysis of cadmium(II) ion in Malee's pineapple juice. Other parameters are the same as in Figure 4.32

Concentration (µM)	%recovery					
	Cd(II) ion					
	1	2	3	average	SD	%RSD
800	99.45	98.25	103.75	100.48	2.89	2.87
600	104.14	105.89	109.79	106.61	2.89	2.71
400	94.98	92.42	99.89	95.76	3.79	3.96
200	109.45	107.01	105.48	107.31	2.00	1.87

4.2.8.3.3 Analysis of copper(II) ion in pine apple juice Malee's

The analysis of copper(II) ion in Malee's pineapple juice with microchip CE and amperometric detection system using the screen-printed carbon electrode is displayed in Figure 4.33. From these results, the relationship between the

current response and the concentration of analyte under the optimum condition. A series of standard solutions with a concentration range of 0 μM to 800 μM was used to determine the linearity of analysis. The results of regression analysis are 0.9972. The %recovery, SD and %RSD from analysis of Cu^{2+} ion in these samples are shown in Table 4.14.
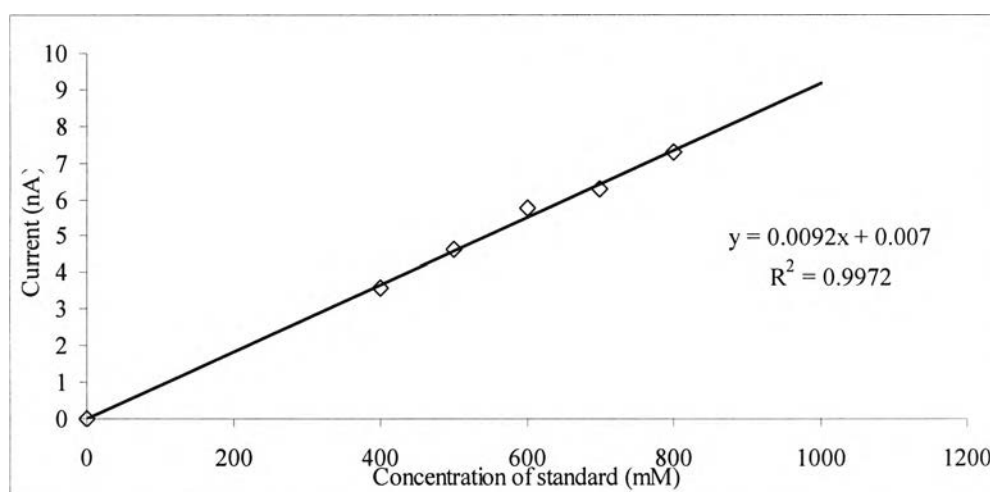
Figure 4.33 The relationship between the peak currents and the concentration of copper(II) ion in Malee's pineapple juice. Experimental parameters: 25 mM MES and L-His pH 7.0 used as running buffer; separation voltage, 1200 V; detection potential, -0.8 V; sampling time, 3 s.

Table 4.14 The %recovery from analysis of copper(II) ion in Malee's pine apple juice. Other parameters are the same as in Figure 4.33

Concentration (μM)	%recovery					
	Cu(II) ion					
	1	2	3	average	SD	%RSD
800	104.03	99.79	100.29	101.37	2.32	2.28
700	98.68	98.91	98.50	98.70	0.20	0.20
600	100.92	104.81	105.11	103.61	2.34	2.25
500	95.88	97.35	100.80	98.01	2.52	2.57
400	91.92	94.61	96.97	94.50	2.52	2.67